Edge magnetoplasmons: low frequency weakly damped excitations in inhomogeneous two-dimensional electron systems

V. A. Volkov and S. A. Mikhailov

Radio Engineering and Electronics Institute, USSR Academy of Sciences
(Submitted 14 July 1987)
Zh. Eksp. Teor. Fiz. **94**, 217–241 (August 1988)

Low frequency collective excitations—the so-called edge magnetoplasmons (EMP)—can propagate along the edge of a $2D$-electron system in a magnetic field. In this paper, we construct from first principles a theory of EMP in various $2D$ systems (heterojunctions, MIS structures and electrons on the surface of liquid helium). We obtain an exact solution to the EMP problem at a sharp rectilinear boundary between two half-planes with differing conductivities. In strong magnetic fields the EMP propagate in a narrow strip near the edge of the system, and are characterized by a gapless spectrum and anomalously weak attenuation. We work out an approximate method of solution for real structures in strong magnetic fields (e.g., for a system with a diffuse edge, for a strip and for a disk). We investigate EMP-like excitations of an inhomogeneous $2D$ system in the quantum Hall effect regime, and determine the EMP contribution to the response of a $2D$ system in an external AC electric field. Our results agree with experimental data.

1. INTRODUCTION

The properties of plasma oscillations in a solid depend on the solid's band structure, the effective dimensions of the sample, the presence of boundaries, and magnetic fields. In the three-dimensional case the plasmon energy (volume and surface) varies from 0.1 eV for doped semiconductors to 10 eV for metals. Three-dimensional plasmon frequencies are large compared to the cyclotron frequency; therefore their properties are only weakly affected by magnetic fields as a rule. The situation is otherwise in the two-dimensional ($2D$) case, which can arise in modulation-doped heterostructures, metal-insulator-semiconductor (MIS) structures, etc. The $2D$ plasmon frequency vanishes in the long-wavelength limit $q \to 0$ (Refs. 2–6):

$$\omega_p(q_x, q_y) = [2\pi n_s e^2 q / m^* \Delta(q)]^{1/2}. \qquad (1)$$

Here $\mathbf{q} = (q_x, q_y)$ is the wave vector of the $2D$-plasmon, n_s and m^* are the number density and effective mass of the $2D$ electrons, and $\Delta(q)$ is a factor which depends on geometry and the dielectric properties of the surrounding media (see Appendix 1).

The magnetic field $\mathbf{B}$ perpendicular to the plane of the $2D$ layer gives rise to a gap in the $2D$ plasmon spectrum equal to the cyclotron frequency $\omega_c = eB/m^*c$. The spectrum of $2D$ magnetoplasmons has the form (Refs. 5,6):

$$\omega_{mp}^2(q) = \omega_c^2 + \omega_p^2(q). \qquad (2)$$

The plasmons are weakly damped only in the collisionless limit ($\omega\tau \gg 1$, where τ is the momentum relaxation time); therefore measurements of (1) and (2) are carried out in the far IR band.

Recently researchers have observed new resonance modes in $2D$ systems whose frequencies are smaller than ω_c [which contradicts (2)]. These frequencies decrease with increasing B, and are located in the far IR, microwave and even radio-frequency ranges (where the condition $\omega\tau > 1$ is violated). The new modes are $2D$ analogues of surface magnetoplasmons; in Ref. 7 they are called "edge magnetoplasmons" (EMP). The number of quantitative theoretical and experimental papers on this topic is already rather large[7–27]; however, the results obtained and their interpretation are very contradictory.

In this paper we will construct a rigorous theory of EMP which applies to all types of $2D$ systems with sharp conductivity profiles near a boundary. The properties of the EMP are expressed in terms of the components of the conductivity tensor of an infinite $2D$ system. We will show that EMP propagate in a narrow strip along the boundary of the $2D$ system, have a gapless spectrum (for half-planes), and have anomalously small attenuation. In light of this last fact, we have paid particular attention to the properties of EMP in the regime of the quantum Hall effect (QHE).[28] Excitations analogous to EMP also exist in infinite but inhomogeneous $2D$ systems in strong magnetic fields.

The complexity of the problem is due fundamentally to the necessity of including the spatial dispersion of the dielectric permittivity in the $2D$ case. Formally the problem of finding the amplitude of the EMP potential in a system with a sharp profile reduces to solving a Wiener-Hopf integral equation with a complicated kernel. Approximate or numerical methods used to solve this equation can lead (and often do lead) to results which are quantitatively or even qualitatively incorrect. The criterion for correctness of such results is comparison with exact results first obtained for a special case in Ref. 11.

Section 2 of this paper is devoted to a qualitative investigation of EMP. The foundation of the paper is Sec. 3, where we present an exact solution to the problem of EMP at a sharp boundary between two half-planes having differing conductivities. An analysis of these general results is contained in Sec. 4 (for electrons in heterostructures), Sec. 5 (for electrons at the surface of liquid helium) and Sec. 6 (for electrons in MIS structures). We also investigate the effects of image forces at the lateral boundary of the $2D$ system on the EMP, of diffusion current, of small-scale fluctuations of the impurity potential in the QHE regime and of the finite thickness of the substrate. In Sec. 7 we propose an approximate method for dealing with more complicated systems, and investigate the following problems: EMP in a strip and a disk, the contribution of EMP to the response of a $2D$ system of finite dimensions in an external AC electric field, and EMP at a diffuse[1] system boundary in strong magnetic fields. In Sec. 8 the results are compared with experiment and with other theoretical papers. A quantum-mechanical interpretation of EMP is given, from which it follows that there exist additional low-frequency modes in a quantizing magnetic field: the so-called acoustic EMP, which have not yet been seen in experiment. Short communications on several results in this paper have been published in Refs. 11, 16, 17, 24.

2. QUALITATIVE INVESTIGATION

The origin of EMP can be viewed in the following way. Let us assume we have a $2D$ electron layer in, e.g., the shape of a disk (Fig. 1a). Suppose that fluctuations appear in the charge density, and therefore in the electric field **E**, within a narrow strip near the edge of the disk. In a strong magnetic field perpendicular to the plane of the disk, when the Hall conductivity σ_{xy} is large compared to the diagonal conductivity σ_{xx}, electrons drift in the direction perpendicular to **E** and **B**, and are stored at the disk's edge; this causes a displacement of the fluctuation along the disk edge (Fig. 1b). Once this happens, the process repeats, leading to a rotation of the fluctuation. This rotational motion occurs at the frequency of the fundamental (Figs. 1a, 1b) or one of the excited (Fig. 1c) EMP modes. In the limit of an infinite-radius disk we arrive at an EMP which travels along the edge of the half-plane (Fig. 1d).

Let us investigate in detail the formation of EMP for a half-plane $\{z=0,\ x\geqslant 0,\ -\infty<y<+\infty\}$ in a magnetic field $\mathbf{B}=(0,0,B)$. Assume the charge is stored near the boundary in a strip of width b, where $b\neq 0$ (the presence of a charged δ-function layer ($b=0$) at the edge of the $2D$ system would lead to a logarithmic divergence of the potential and electrostatic energy[29]; in the $3D$ case, in contrast to the $2D$ case, the charge of a surface plasmon can be concentrated in a δ-function layer at the sample surface when we neglect spatial dispersion[30]). The EMP potential

$$\varphi(x,y,z,t)=\varphi(x,z)\exp(iq_y y-i\omega t)$$

is determined by the amplitude of the linear charge density Q:

$$\varphi(x,z=0)\approx\frac{2Q}{\tilde{\varkappa}}\ln\frac{1}{|q_y|x}\qquad b\ll x\ll|q_y|^{-1},\tag{3}$$

where $\tilde{\varkappa}$ is the mean dielectric permittivity of the surrounding media, and q_y is the EMP wave vector. The magnitude of Q is controlled by the current which leaks into the strip:

$$i\omega Q=j_x(x\sim b).$$

In a strong magnetic field ($|\sigma_{xx}/\sigma_{xy}|\ll 1$),

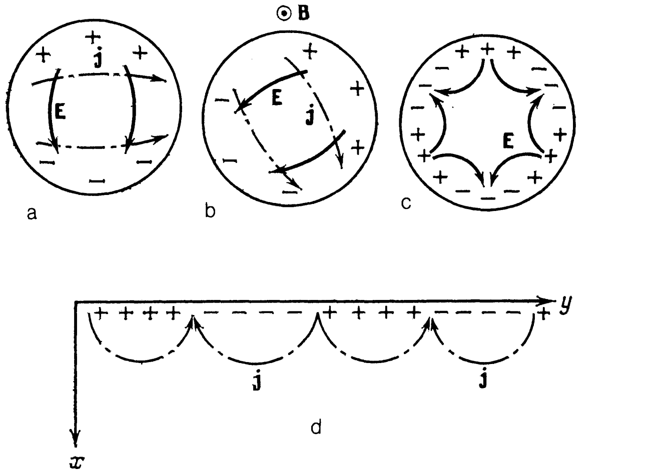

FIG. 1. Distributions of charge,field **E**, and current **j** for the fundamental (dipole) EMP mode at an initial (a) and subsequent (b) instant of time; (c) shows the charge distribution and field of the $n=3$ EMP mode; (d) shows the charge and current distributions for an EMP wave in a semi-infinite ($x>0$) $2D$ layer (the picture moves with time in the $+y$ direction).

$$j_x\approx-iq_y\sigma_{xy}\varphi(x,z=0).$$

The self-consistent EMP potential (3) takes the form

$$\varphi(x,z=0)\approx-\frac{2q_y\sigma_{xy}}{\omega\tilde{\varkappa}}\varphi(x\sim b,z=0)\ln\frac{1}{|q_y|x}\qquad b\ll x\ll|q_y|^{-1}.\tag{4}$$

Setting $x\sim b$, we obtain the EMP spectrum for a half-plane when $|q_y|b\ll 1$:

$$\operatorname{Re}\omega(q_y)\equiv\omega'(q_y)=-\frac{2q_y\sigma_{xy}}{\tilde{\varkappa}}\left[\ln\frac{1}{|q_y|b}+O(1)\right].\tag{5}$$

The attenuation $\omega''(q_y)\equiv\operatorname{Im}\omega(q_y)$ is determined by the resorption time of the EMP charge under the action of the field E_x, i.e., the Maxwell time, which depends in the $2D$ case on the wave vector:

$$\omega''(q_y)\sim-2\pi\sigma_{xx}'|q_x|/\tilde{\varkappa},$$

where $\sigma_{xx}'=\operatorname{Re}\sigma_{xx}$. The length $|q_x|^{-1}$ over which the electric field of the EMP forms ($|q_x|^{-1}\ll|q_y|^{-1}$), is estimated from the condition that the normal current vanish at the edge of the system (which follows from the absence of charged δ-function layers for $x=0$): $q_x\sigma_{xx}+q_y\sigma_{xy}=0$. From this it follows that

$$\omega''(q_y)\sim-\frac{2\pi|q_y\sigma_{xy}|}{\tilde{\varkappa}}\frac{\sigma_{xx}'}{|\sigma_{xx}'+i\sigma_{xx}''|}.\tag{6}$$

The components of the conductivity tensor at the EMP frequency enter into (5), (6). Because $\sigma'_{\alpha\beta}\equiv\operatorname{Re}\sigma_{\alpha\beta}$ is an even and $\sigma''_{\alpha\beta}\equiv\operatorname{Im}\sigma_{\alpha\beta}$ an odd function of ω, for small ω we can limit ourselves to the first terms of the expansion of $\sigma_{\alpha\beta}(\omega)$ for $\omega/\omega_0\ll 1$:

$$\sigma_{xx}'(\omega)\approx\sigma_{xx}'(0),\quad\sigma_{xx}''(\omega)\approx-\sigma_{xx}'(0)\omega\tau^*,\quad\sigma_{xy}(\omega)\approx\sigma_{xy}(0),\tag{7}$$

where we have introduced a real parameter τ^* with the dimensions of time and a characteristic frequency ω_0 which determines the dispersion of $\sigma_{\alpha\beta}(\omega)$. In the Drude model the time τ^* in a strong field B (i.e., $\omega_c \gg |\omega + i/\tau|$) reduces to the elastic relaxation time τ, while the role of ω_0 is played by ω_c. In the QHE regime, ω_0 has the meaning of a characteristic frequency for motion of impurity electrons localized by the field[31]; experiments[32,33] suggest the estimate $\omega_0/2\pi > 35$ GHz.

In the low-frequency limit ($\omega\tau^* \ll 1$) we obtain from (6), (7)

$$\omega''(q_y) \sim -2\pi |q_y \sigma_{xy}|/\varkappa, \tag{8}$$

i.e., the EMP decay does not depend on the dissipative component of the conductivity σ'_{xx} and is quantized in the QHE regime. In the high-frequency limit ($\omega\tau^* \gg 1$)

$$\omega''(q_y) \sim -\frac{2\pi |q_y \sigma_{xy}|}{\varkappa |\omega\tau^*|} \sim -\frac{\pi}{\tau^*}\left[\ln\frac{1}{|q_y| b}\right]^{-1}. \tag{9}$$

But what determines the length b which enters into (5) and (9)? It follows from the exact solution (Sec. 3) that for an infinitely thin $2D$ layer with a sharp boundary the role of b is played by a length $|l|$:

$$l = 2\pi i \sigma_{xx}(\omega)/\varkappa\omega = l_0 + i l_1, \tag{10}$$

where

$$l_0 = -2\pi\sigma_{xx}''(\omega)/\omega\varkappa, \quad l_1 = 2\pi\sigma_{xx}'/\omega\varkappa,$$

$|l| \approx l_0$ for $\omega\tau^* \gg 1$ and $|l| \approx l_1$, for $\omega\tau^* \ll 1$. The physical meaning of l_0 is clarified in the Drude model for $\omega \ll |\omega_c + i/\tau|$:

$$l_0 = 2\pi n_s e^2/m^*\varkappa\omega_c^2 = e^2\nu/\varkappa\hbar\omega_c. \tag{11}$$

For $\nu \sim 1$, l_0 determines the distance over which the electron-electron interaction energy is comparable to the cyclotron energy (ν is the degree of degeneracy of the Landau level).

In taking into account the finite thickness d_{2D} of the $2D$ layer and the diffuseness of the edge (h is the width of the region over which the $2D$ electron concentration changes near $x = 0$), the role of b is played by the maximum of the lengths l_0, l_1, d_{2D}, and h.

For $\omega \to 0$ (to be precise, $\omega\tau^* \ll 1$ and $b \approx l_1$), after iterating (5) we obtain

$$\omega'(q_y) \sim -\frac{2q_y\sigma_{xy}}{\varkappa}\ln\frac{|\sigma_{xy}(0)|}{\sigma_{xx}'(0)}. \tag{12}$$

In the QHE regime $\sigma'_{xx}(0)$ depends exponentially on the electron temperature T; therefore the EMP frequency (12) is a power-law function of T, while the EMP attenuation is independent of T.

In a sample with finite dimensions the wave vector of the EMP takes on discrete values. If the length b is small compared to the sample dimensions (along the x and y axes), which should hold in a sufficiently strong magnetic field, we can expect that the results obtained above remain valid if we understand q_y to be the quantity

$$q_y = 2\pi n/P, \tag{13}$$

where P is the sample perimeter, and $n = \pm 1, \pm 2, \ldots$. From (5) and (13) there follows an estimate of the frequency of the fundamental EMP mode ($\omega/2\pi \sim 0.1$–10 GHz for typical heterostructure parameters and $P \sim 1$ cm), which justifies the expansion (7) even in the QHE regime.

These illustrations allow us to understand some important properties of EMP: (1) Their frequency is determined by the slow (Hall) motion of the electrons ($\omega \propto \sigma_{xy} \propto B^{-1}$) and can be very small compared to $\omega_c \propto B$; (2) the low-frequency EMP propagates only in one direction along the edge of the system, determined by the vector $e\mathbf{B}\times\mathbf{N}$, where $\mathbf{N}$ is the outward normal to the boundary of the $2D$ system in the plane $z = 0$; (3) in a strong magnetic field the Hall current dominates over the dissipative current and the EMP is weakly attenuated ($\omega' > \omega''$) not only for $\omega\tau^* \gg 1$, but also for $\omega\tau^* \ll 1$; (4) the appearance of EMP is closely related to the Hall effect; therefore ω' and ω'' can take on quantized values in the QHE regime.

3. AN EXACTLY SOLUBLE EMP PROBLEM

Let us investigate a $2D$ layer (the plane $z = 0$) whose conductivity tensor in a field $\mathbf{B} = (0,0,B)$ changes discontinuously at $x = 0$:

$$\sigma_{\alpha\beta}(\mathbf{r}, \omega) = \{\sigma_{\alpha\beta}{}^L(\omega) + [\sigma_{\alpha\beta}{}^R(\omega) - \sigma_{\alpha\beta}{}^L(\omega)]\theta(x)\}\delta(z)$$
$$\equiv \sigma_{\alpha\beta}(z, \omega)\delta(z). \tag{14}$$

Here, $(\alpha,\beta) = (x,y)$, $\sigma_{xx} = \sigma_{yy}$, $\sigma_{xy} = -\sigma_{yx}$, $\sigma_{zz} = 0$; $\theta(x) = 1$ for $x > 0$, $\theta(x) = 0$ for $x < 0$; the superscript L (R) denotes the left (right) half-plane; in the special case of a semi-infinite ($x \geqslant 0$) $2D$ layer $\sigma^L_{\alpha\beta} = 0$, $\sigma^R_{\alpha\beta} \neq 0$. Oscillations of the charge density $\rho(\mathbf{r},t)$, the current density $\mathbf{j}(\mathbf{r},t)$ and potential $\varphi(\mathbf{r},t)$ in a plasma wave propagating along the line $x = z = 0$ (the internal "edge" of the system) satisfy the following system of differential equations in $3D$ space:

$$\nabla[\varkappa(z)\nabla\varphi] = -4\pi\rho,$$
$$\partial\rho/\partial t + \operatorname{div}\mathbf{j} = 0, \quad j_\alpha = -\sigma_{\alpha\beta}\nabla_\beta\varphi$$

with the boundary condition

$$\lim_{|\mathbf{r}|\to\infty}\varphi(\mathbf{r}, t) = 0,$$

where $\varkappa(z)$ is the local dielectric permittivity of the surrounding medium. Let us seek a continuous and bounded solution $\varphi(\mathbf{r},t)$. We assume

$$\varphi, \mathbf{j}, \rho \propto \exp(iq_y y - i\omega t)$$

and after writing the Poisson equation in its integral form, we obtain equations for the amplitudes $\varphi(x,z)$ and $\rho(x,z)$:

$$\varphi(x, z) = 4\pi\iint dx'\,dz'\,G_{q_y}(x-x'; z, z')\rho(x', z'),$$
$$\rho(x, z) = -\frac{\delta(z)}{i\omega}\left\{\frac{\partial}{\partial x}\left(\sigma_{xx}\frac{\partial}{\partial x}\right) - q_y{}^2\sigma_{xx} + iq_y\frac{\partial\sigma_{xy}}{\partial x}\right\}\varphi(x, z), \tag{15}$$

where G_{q_y} $(x - x'; z,z')$ is the Fourier transform of the Green's operator $\nabla[\varkappa(z)\nabla]$. By eliminating ρ from (15), integrating (14) by parts and setting $z = 0$, we are led to an integrodifferential equation of Wiener-Hopf type for $\varphi(x)\equiv\varphi(x,0)$:

$$\varphi(x)=-\frac{4\pi}{i\omega}\left\{\left(\frac{\partial^2}{\partial x^2}-q_y^2\right)\int_{-\infty}^{+\infty}G_{q_y}(x-x';0,0)\sigma_{xx}\right.$$

$$(x',\omega)\varphi(x')\,dx'$$

$$\left.+\varphi(0)\left[iq_y(\sigma_{xy}{}^R-\sigma_{xy}{}^L)-(\sigma_{xx}{}^R-\sigma_{xx}{}^L)\frac{\partial}{\partial x}\right]G_{q_y}(x;0,0)\right\}. \quad (16)$$

In order to solve (16) we introduce the functions $\varphi_\pm(x)=\theta(\pm x)\varphi(x)$, whose Fourier transforms

$$\Phi_\pm(q_x)=\int_{-\infty}^{+\infty}\varphi_\pm(x)e^{iq_xx}\,dx$$

are analytic in the upper (Φ_+) and lower (Φ_-) q_x half planes. With the help of a Fourier transform we are led to the form

$$\Phi_+(q_x)\varepsilon^R(q_x)+\Phi_-(q_x)\varepsilon^L(q_x)$$

$$=-\varphi(0)\frac{q_y\,\delta\sigma_{xy}+q_x\,\delta\sigma_{xx}}{i\delta\sigma_{xx}(q_x^2+q_y^2)}[\varepsilon^R(q_x)-\varepsilon^L(q_x)], \quad (17)$$

where $\delta\sigma_{\alpha\beta}=\sigma^R_{\alpha\beta}-\sigma^L_{\alpha\beta}$, $G(q_x,q_y)$ is the Fourier-transform of the function $G_{q_y}(x;0,0)$, while

$$\varepsilon^{R,L}(q_x)=1+\frac{4\pi i\sigma_{xx}^{R,L}(\omega)}{\omega}q^2G(q_x,q_y) \quad (18)$$

is the longitudinal dielectric permittivity of an infinite $2D$ layer with conductivity σ^R_{xx} or σ^L_{xx}. The explicit form of $\varepsilon(q_x)$ for various cases is presented in Appendix 1.

In order to find functions Φ_+ (Φ_-) which are analytic in the upper (lower) q_x half planes and which satisfy condition (17) on the real axis (the Riemann boundary value problem[34]), we introduce the functions

$$X_\pm(q_x)=\exp\left\{-\frac{1}{2\pi i}\int_{-\infty}^{+\infty}\frac{dq_x'}{q_x'-q_x\mp i0}\ln\frac{\varepsilon^R(q_x')}{\varepsilon^L(q_x')}\right\}, \quad (19)$$

which are analytic and have no zeroes in the upper (X_+) or lower (X_-) q_x half-planes (see Appendix 2). Using the identity

$$\varepsilon^R(q_x)/\varepsilon^L(q_x)=X_-(q_x)/X_+(q_x), \quad (20)$$

which follows from the definition (19), we rewrite (17) in a more convenient form:

$$\frac{\Phi_+(q_x)}{X_+(q_x)}+\frac{\Phi_-(q_x)}{X_-(q_x)}$$

$$=-\varphi(0)\frac{q_y\delta\sigma_{xy}+q_x\delta\sigma_{xx}}{i\delta\sigma_{xx}(q_x^2+q_y^2)}\left[\frac{\varepsilon^R(q_x)-\varepsilon^L(q_x)}{\varepsilon^L(q_x)X_-(q_x)}\right]. \quad (21)$$

Casting the right side of (21) in the form of a difference of the functions Ψ_+ and Ψ_-,

$$\Psi_\pm(q_x)=\frac{1}{2\pi i}\int_{-\infty}^{+\infty}\frac{dq_x'}{q_x'-q_x\mp i0}\frac{q_y\delta\sigma_{xy}+q_x'\delta\sigma_{xx}}{i\delta\sigma_{xx}(q_x'^2+q_y^2)}$$

$$\cdot\left[\frac{\varepsilon^R(q_x')-\varepsilon^L(q_x')}{\varepsilon^L(q_x')X_-(q_x')}\right], \quad (22)$$

which are analytic in the upper (Ψ_+) or lower (Ψ_-) half-planes, we obtain

$$\Phi_+(q_x)/X_+(q_x)+\varphi(0)\Psi_+(q_x)$$

$$=-\Phi_-(q_x)/X_-(q_x)+\varphi(0)\Psi_-(q_x). \quad (23)$$

The left (right) side of (23) is the boundary value of a function analytic in the upper (lower) half-plane q_x. According to a theorem on analytic continuation and the generalized Liouville theorem, under the supplementary requirement that $\Phi_\pm(q_x\to\infty)=0$, which is a consequence of the condition that $\varphi(0)$ be finite, both sides of (23) are identically zero.[34] Therefore

$$\Phi_\pm(q_x)=\mp\varphi(0)X_\pm(q_x)\Psi_\pm(q_x). \quad (24)$$

Up until now we have followed the general program of the Wiener-Hopf method. For further progress we turn to a specific problem. Let us first note that by taking (20) into account we can cast the combination of functions which stand in the square brackets in (22), and which have branch points at $\pm i|q_y|$, in the form of a difference of two functions which are analytic in their corresponding half-planes:

$$[\varepsilon^R(q_x)-\varepsilon^L(q_x)]/\varepsilon^L(q_x)X_-(q_x)=1/X_+(q_x)-1/X_-(q_x).$$

Therefore the right side of (22) is a difference of two integrals. In the integral containing X_+ (X_-), we shift the contour of integration into the upper (lower) half-plane and use the residue theorem at the simple poles $q_x\pm i0$, $\pm i|q_y|$. Expression (24) is then greatly simplified:

$$\Phi_\pm(q_x)=\mp\frac{\varphi(0)}{i\delta\sigma_{xx}}\left\{\frac{q_y\delta\sigma_{xy}+q_x\delta\sigma_{xx}}{q_x^2+q_y^2}\right.$$

$$\left.+\frac{X_\pm(q_x)}{2i|q_y|}\left[\frac{A_-}{q_x+i|q_y|}-\frac{A_+}{q_x-i|q_y|}\right]\right\}, \quad (25)$$

where

$$A_\pm=(q_y\delta\sigma_{xy}\pm i|q_y|\delta\sigma_{xx})/X_\pm(\pm i|q_y|). \quad (26)$$

The functions $\varphi_\pm(x)$ which are discontinuous at $x=0$ are integrals of the Fourier functions (25). Their values at the point $x=0$ are obtained by integrating over the infinite half-circles in the upper (φ_+) and lower (φ_-) q_x half planes:

$$\varphi_\pm(x\to\pm0)=2\varphi_\pm(0)=\mp\frac{\varphi(0)}{\pi i\delta\sigma_{xx}}\int_{-\infty}^{+\infty}dq_x\left\{\frac{q_y\delta\sigma_{xy}+q_x\delta\sigma_{xx}}{q_x^2+q_y^2}\right.$$

$$\left.+\frac{X_\pm(q_x)}{2i|q_y|}\left[\frac{A_-}{q_x+i|q_y|}-\frac{A_+}{q_x-i|q_y|}\right]\right\}$$

$$=\varphi(0)\left\{1+\frac{X_\pm(\pm i\infty)}{2i|q_y|\delta\sigma_{xx}}[A_--A_+]\right\}.$$

We require continuity of $\varphi(x)$ at $x=0$. Then

$$A_+=A_-\equiv A. \tag{27}$$

Transforming (27) and taking into account (26), (19) and (A6), we finally obtain the exact dispersion relation for determining the EMP spectrum $\omega(q_y)$:

$$1+\frac{q_y\delta\sigma_{xy}}{i|q_y|\delta\sigma_{xx}}\tanh\left\{\frac{1}{\pi}\int_0^\infty\frac{d\xi}{1+\xi^2}\ln\left[\frac{\varepsilon^R(q,\omega)}{\varepsilon^L(q,\omega)}\right]_{q_x=|q_y|\xi}\right\}=0. \tag{28}$$

The case of an EMP for a half-plane ($\sigma^L_{\alpha\beta}=0$, $\sigma^R_{\alpha\beta}=\sigma_{\alpha\beta}\neq 0$) requires a special investigation, because $X_+(q_x\to\infty)=0$, $X_-(q_x\to\infty)\to\infty$. In this case condition (27) and consequently (28) (see Ref. 11) follow from the finiteness of $\varphi_-(x)$ as $x\to -0$.

It is not difficult to show that (28) also describes the spectrum $\omega(q_y,q_z)$ of EMP which propagate along the lateral boundary $x=0$ of a superlattice whose axis coincides with the z axis and which has the dielectric function (A5).

The EMP potential, taking (27) into account, is described by the expressions

$$\varphi_\pm(x)=\mp\frac{\varphi(0)}{2\pi i\delta\sigma_{xx}}\int_{-\infty}^{+\infty}\frac{dq_xe^{-iq_xx}}{q_x^2+q_y^2}\{q_y\delta\sigma_{xy}+q_x\delta\sigma_{xx}-AX_\pm(q_x)\}, \tag{29}$$

from which we obtain the value of the EMP electric field at $x=\pm 0$:

$$\left.\frac{\partial\varphi_\pm}{\partial x}\right|_{x=\pm 0}=\frac{\varphi(0)}{2i\delta\sigma_{xx}}[2q_y\delta\sigma_{xy}-AX_\pm(\pm i\infty)]. \tag{30}$$

From (30) it follows that the normal component j_x of the EMP current is continuous at the boundary $x=0$. In the case $\sigma^L_{\alpha\beta}=0$ the normal current $j_x(x=+0)=0$, which was obtained by another method in Sec. 2, while the EMP field diverges for $x\to -0$ but is finite as $x\to +0$:

$$\partial\varphi_+/\partial x|_{x=+0}=\varphi(0)\,q_y\sigma_{xy}{}^R/i\sigma_{xx}{}^R. \tag{31}$$

We now bring in the exact expressions for the charge density

$$\rho(x)=\theta(x)\rho_+(x)+\theta(-x)\rho_-(x),$$

the linear charge density $Q_\pm$, and also the charge and characteristic length over which the amplitude of the EMP potential decreases in "center of gravity" coordinates for $\sigma^L_{\alpha\beta}=0$:

$$\rho_\pm(x)=\pm\varphi(0)\frac{A\sigma_{xx}(x)}{i\omega\delta\sigma_{xx}}\frac{1}{2\pi i}\int_{-\infty}^{+\infty}dq_xX_\pm(q_x)e^{-iq_xx}, \tag{32}$$

$$Q_\pm\equiv\pm\int_0^{\pm\infty}\rho_\pm(x)\,dx$$

$$=\mp\varphi(0)\frac{A\sigma_{xx}(x)}{\omega\delta\sigma_{xx}}\left[X_\pm(0)-\frac{1}{2}X_\pm(\pm i\infty)\right], \tag{33}$$

$$Q_+{}^{-1}\int_0^\infty x\rho_+(x)\,dx=-i\left.\frac{\partial\ln X_+(q_x)}{\partial q_x}\right|_{q_x=0},$$

$$\delta_\varphi\equiv\frac{1}{\varphi(0)}\int_0^\infty\varphi_+(x)\,dx=\frac{i\sigma_{xy}}{q_y\sigma_{xx}}\left\{1-\frac{A}{q_y\sigma_{xy}}X_+(0)\right\}. \tag{34}$$

Here $\sigma_{xx}(x)=\sigma^R_{xx}$ for ρ_+, Q_+, and $\sigma_{xx}(x)=\sigma^L_{xx}$ for ρ_-, Q_-. Equation (32) clarifies the meaning of the functions $X_\pm(q_x)$ which were introduced into (19): they are proportional to the Fourier components of the charge density.

Up until now we have assumed that the background dielectric permittivity $\varkappa(z)$ does not depend on x and y. If $\varkappa=\varkappa(x,z)$, then it is necessary to include the influence of the image charges which arise near the lateral boundary $x=0$ on the EMP spectrum. When the half-space $x>0$ ($x<0$) is occupied by a dielectric with permittivity $\varkappa^R$ ($\varkappa^L$), $\sigma_{\alpha\beta}(x,\omega)=\theta(x)\sigma^R_{\alpha\beta}(\omega)$ and $\sigma^L_{\alpha\beta}=0$, it is not difficult to obtain a generalization of Eq. (16):

$$\varphi(x)=\frac{4\pi i\sigma_{xx}{}^R}{\omega}\left[1+\alpha\theta(-x)\right]\left(\frac{\partial^2}{\partial x^2}-q_y{}^2\right)\int_0^\infty dx'\varphi(x')$$

$$\cdot[G_{q_y}(x-x';0,0)+\alpha\theta(x)G_{q_y}(x+x';0,0)]$$

$$-\frac{4\pi\varphi(0)}{i\omega}[1+\alpha\theta(-x)]$$

$$\cdot\left\{iq_y\sigma_{xy}{}^R[1+\alpha\theta(x)]-\sigma_{xx}{}^R[1-\alpha\theta(x)]\frac{\partial}{\partial x}\right\}G_{q_y}(x;0,0), \tag{35}$$

which describes the amplitude of the EMP potential for a heterojunction or superlattice (the latter if we replace G_{q_y} by $G_{g_y g_z}$). An exact solution to (35) for arbitrary values of $\alpha=(\varkappa^R-\varkappa^L)/(\varkappa^R+\varkappa^L)$ is not known. However, in experiments we usually find that $\varkappa^R\gg\varkappa^L$, and we can then assume that $\alpha=1$. The method of solving the equation obtained from (35) with $\alpha=1$ is discussed in Ref. 35. By direct substitution we can show that the Fourier transform of the function $\varphi_+(x)=\theta(x)\varphi(x)$ has the form

$$\Phi_+(q_x)=\frac{q_y\sigma_{xy}{}^R\varphi(0)}{\pi\sigma_{xx}{}^R}\int_{-\infty}^{+\infty}\frac{dq_x'}{q_x'-q_x-i0}\left[\frac{\varepsilon^R(q_x')-1}{\varepsilon^R(q_x')\,(q_x'^2+q_y^2)}\right]. \tag{36}$$

Again after computing $\varphi_+(x\to +0)\equiv\varphi(0)=2\varphi_+(0)$, we obtain the dispersion relation for the EMP for $\alpha=1$:

$$1+\frac{q_y\sigma_{xy}{}^R}{i|q_y|\sigma_{xx}{}^R}\frac{1}{\pi}\int_{-\infty}^{+\infty}\frac{d\xi}{1+\xi^2}\left[1-\frac{1}{\varepsilon^R(q,\omega)}\right]_{q_x=|q_y|\xi}=0, \tag{37}$$

where ε^R is given by (A1) or (A2).

Let us turn now to an analysis of these results.

4. EMP IN HETEROSTRUCTURES

Let us investigate the properties of EMP in a $2D$ electron system with dielectric function (A1) and a sharp profile for $\sigma_{\alpha\beta}(x)$.

Edge plasmons in zero magnetic field. For $\sigma^L_{\alpha\beta}=0$,

$B = 0$ ($\sigma_{xy}^{R,L} = 0$) edge plasmons can propagate along the $x = 0$ boundary of the system with a spectrum $\omega(q_y)$ determined by an equation derivable from (28):

$$\mathrm{ch}\left\{\frac{1}{\pi}\int_0^\infty \frac{d\xi}{1+\xi^2}\ln \varepsilon(q_x=|q_y|\xi, q_y, \omega)\right\}=0. \qquad (38)$$

In the collisionless approximation ($\sigma_{xx} = in_s e^2/m^*\omega$, $\omega\tau = \infty$), (38) has the unique solution

$$\omega^2(q_y)=\omega_p^2(0, q_y)/\eta_0, \qquad (39)$$

where $\eta_0 = 1.217...$ is a root of the equation

$$\int_0^{\pi/2} dx \ln\left\{\frac{\eta_0}{\sin x}-1\right\}=0,$$

and $\omega_p(q_x), q_y$ is the $2D$ plasmon frequency (1), $\Delta(q) = \varkappa$. Thus, the edge plasmon branch is split off from the edge of the $2D$ plasmon continuum by 10%; $\omega(q_y) \approx 0.906\ \omega_p(0,q_y)$. For $\omega\tau \lesssim 1$ the edge plasmon is strongly damped. The penetration depth of its field into the sample is determined according to (29) by the zero q_{x0} of $\varepsilon(q_x)$ which is closest to the real axis in the lower half-plane; for $|q_{x0}|x > 1$ we have

$$\varphi(x) \propto \exp(-q_{x0}x), \quad q_{x0}=-i|q_y|(1-\eta_0^{-2})^{1/2}\approx -i|q_y|\cdot 0.570.$$

EMP spectrum for a half-plane ($\sigma_{\alpha\beta}^L = 0$). The dispersion relation (28) for $B \neq 0$, $\sigma_{\alpha\beta}^L = 0$, $\sigma_{\alpha\beta}^R \equiv \sigma_{\alpha\beta}$ can be rewritten in the form

$$\omega=-2q_y\sigma_{xy}(\omega)F_1(|q_y|l)/\varkappa,$$

$$F_1(z)=\frac{\pi}{z}\tanh\left\{\frac{1}{\pi}\int_0^{\pi/2} dt\ln\left(1+\frac{z}{\sin t}\right)\right\}. \qquad (40)$$

The length l defined by (10) in the collisionless approximation is real:

$$|q_y|l=\omega_p^2(0, q_y)/(\omega_c^2-\omega^2).$$

In this case Eq. (40) has a real solution in the region $\omega^2 < \omega_{mp}{}^2(0,q_y)$ [see (2)]. Study of the function $F_1(z)$ shows (see Appendix 3) that the EMP spectrum consists of two branches, $\omega_+(q_y)$ and $\omega-(q_y)$, which are labelled with the sign of their phase velocities (Fig. 2a). The right-hand branch $\omega_+(q_y)$ is gapless; we note that $\omega_+(q_y) = \omega_c$ for $q_y = 2/l_0$, where l_0 is defined in (11). The $\omega-(q_y)$ branch exists for $\omega > \omega^* = \omega_c$ cth $(2G/\pi) \approx 1.905\omega_c$, $|q_y| > q_y^* = l_0^{-1}$ [sh $(2G/\pi)]^{-2} \approx 2.627 l_0^{-1}$, where $G = 0.916$ is Catalan's constant. For $\omega = \omega^*$, $q_y = -q_y^*$, the $\omega-(q_y)$ branch enters into the continuum region of $\omega_{mp}(q_x, q_y)$.

Switching on the magnetic field thus leads to a splitting of the edge plasmon frequencies (Fig. 2b). In weak fields ($\omega_c \ll \omega(q_y)$) this splitting can be determined from the relation

$$\omega_\pm^2(q_y) \approx \frac{\omega_p^2(0, q_y)}{\eta_0}-\frac{\pi(\eta_0^2-1)^{1/2}}{\eta_0^{1/2}\arccos(-\eta_0^{-1})}\omega_c\omega_p(0, q_y)\,\mathrm{sign}\,q_y.$$

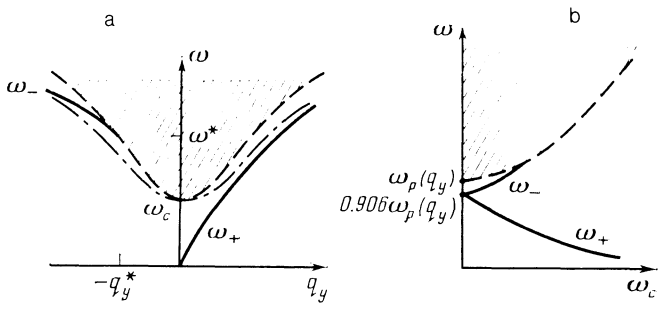

FIG. 2. The EMP frequencies ω_+, ω_- as functions of (a) wave vector for $B =$ const., and (b) magnetic field for $q_y =$ const.; note that $\omega(q_y) = -\omega(-q_y)$. Dashed curve—the boundary of the continuum region of the $\omega_{mp}(q_x, q_y)$ spectrum (which is crosshatched). The dot-dashed curve in (a) is a plot of $[\omega_c^2 + (0.906\ \omega_R(0,q_y))^2]^{1/2}$.

Let us analyze the properties of the right-hand branch in the long-wavelength and low-frequency limit without using the Drude model. Equation (40) simplifies for $|q_y l| \ll 1$:

$$\omega=-\frac{2q_y\sigma_{xy}(\omega)}{\varkappa}\left[\ln\frac{2}{|q_y|l}+1+o(1)\right], \qquad (41)$$

the discarded term in the brackets has the form

$$z^2[\ln(2/z)-1/6-2\pi^{-2}(1+\ln(2/z))^3]/6,$$

where $z = |q_y|l$, and for $|z| \leqslant 1$ gives a correction $\leqslant 4.5\%$. The solution to (41) we obtain by iteration, using the small-ω limit for $\sigma_{\alpha\beta}(\omega)$ and l [see (7), (10)]:

$$\omega_+(q_y)\approx-\frac{2q_y\sigma_{xy}(0)}{\varkappa}\ln\frac{5.436}{|q_y|l_0}-\frac{i}{\tau^*}\left[\ln\frac{5.436}{|q_y|l_0}\right]^{-1},$$

$$|\omega_+|\tau^*\gg 1, \qquad (42)$$

$$\omega_+(q_y)\approx-\frac{2q_y\sigma_{xy}(0)}{\varkappa}f\left(\frac{5.436|\sigma_{xy}(0)|}{\pi\ \sigma_{xx}'(0)}\right)-i\frac{\pi|q_y\sigma_{xy}|}{\varkappa},$$

$$|\omega_+|\tau^*\ll 1. \qquad (43)$$

The function $f(x)$ is the solution of the equation $f(x) = \ln[xf(x)]$; for $|\sigma_{xy}/\sigma_{xx}'| \gg 1$ it is the limit of the following sequence of functions $f_n(x)$ defined by [$f_0(x) = \ln x$, $f_{n+1}(x) = \ln[xf_n(x)]$, which yields $f(x) \approx \ln[x \ln x] + O(\ln\ln x/\ln x)$ for $x \gg 1$.] The rigorous results (42), (43) agree with the qualitative results (5), (8) if we set $b \sim |l|$.

Distributions of potential, field, charge and current for the low-frequency EMP mode $\omega_+(q_y)$ for $\sigma_{\alpha\beta}^L = 0$ in the limits $|q_y l| \ll 1$ and $|\sigma_{xx}'/\sigma_{xy}| \ll 1$. The potential distribution is determined from Eq. (29), which, when (20) and $\varepsilon^L = 1$, $\varepsilon^R(q_x) \equiv \varepsilon(q_x)$ are taken into account, has the form

$$\varphi_\pm(x)=\mp\frac{\varphi(0)}{2\pi i\sigma_{xx}}\int_{-\infty}^{+\infty}\frac{dq_x e^{-iq_x x}}{q_x^2+q_y^2}\{q_y\sigma_{xy}+q_x\sigma_{xx}-AX_\mp(q_x)\varepsilon^{\mp1}(q_x)\}.$$

$$(44)$$

The value of the integral (44), in which we shift the integration contour into the lower (upper sign) or upper (lower sign) q_x half-plane, is determined by the branch points

$(\pm i|q_y|)$ and zeroes (poles) of the function $\varepsilon(q_x)$. The latter are absent for $\omega^2 < \omega_c^2$. Therefore, in the limit $|q_y l| \ll 1$ Eq. (44) and the analogous Eq. (32) reduce to integrals along the cuts $(\pm i|q_y|, \pm i\infty)$:

$$\varphi_\pm(x) = -\frac{2\varphi(0)A}{\omega\tilde{\varkappa}} \int_1^\infty \frac{d\xi}{(\xi^2-1)^{1/2}} \frac{e^{-|q_y|x\xi} X_\mp(\mp i|q_y|\xi)}{1+\theta(x)(q_y l)^2(\xi^2-1)},$$
$$\rho_+(x) = -\frac{\varphi(0)A q_y^2 l}{\pi\omega} \int_1^\infty \frac{d\xi\,(\xi^2-1)^{1/2} X_-(-i|q_y|\xi)\, e^{-|q_y|x\xi}}{1+(q_y l)^2(\xi^2-1)}. \tag{45}$$

Taking into account that in the limit in question $A \approx q_y \sigma_{xy}$, we obtain the asymptotic forms of (45):

$$\varphi_\pm(x) \approx \varphi(0)\frac{1}{S} K_0(|q_y|x), \qquad |x| \gg |l|/\pi, \tag{46a}$$

$$\varphi_+(x) = \varphi(0)\left\{1 - \frac{1}{S}\left[\frac{\pi x}{l} - \frac{4}{3\pi}\left(\frac{\pi x}{l}\right)^{3/2} + \ldots\right]\right\}, \qquad x \to +0, \tag{46b}$$

$$\varphi_-(x) = \varphi(0)\left\{1 - \frac{2}{S}\left(-\frac{\pi x}{l}\right)^{1/2} + \ldots\right\}, \qquad x \to -0, \tag{46c}$$

$$\rho_+(x) \approx \varphi(0)\frac{\tilde{\varkappa}|q_y|l}{2\pi S}\frac{1}{x}K_1(|q_y|x), \qquad x \gg |l|/\pi, \tag{46d}$$

$$\rho_+(x) = \varphi(0)\frac{\tilde{\varkappa}}{2lS}\left(\frac{l}{\pi x}\right)^{1/2} + \ldots, \qquad x \ll |l|/\pi. \tag{46e}$$

Here, $S \equiv -\omega\tilde{\varkappa}/2q_y\sigma_{xy}$ is the dimensionless phase velocity of the EMP, $K_n(z)$ is the nth order modified Bessel function of the second kind ($K_1(z) = -K_0'(z)$, $K_0(z) \approx \ln(2/z) - C$ for $z \ll 1$, $K_0(z) \approx (\pi/2z)^{1/2}\exp(-z)$ for $z \gg 1$; $C = 0.577\ldots$ is Euler's constant). The rigorous result (46a) coincides with the qualitative result (5).

Our analysis shows that for $|q_y l| \ll 1$ the EMP charge is concentrated primarily near the edge in a strip whose width is on the order of $|l|$, which validates the qualitative arguments in Sec. 2. The "center of gravity" of the charge (33) for $|q_y l| \ll 1$ is found at the point $(l/\pi)\ln(2/|q_y|l)$.

The components of the field and current are found by differentiating (45) or (46a), (46b) (see Fig. 3). The EMP field decreases algebraically for $x \lesssim |q_y|^{-1}$ and exponentially for $x > |q_y|^{-1}$. The characteristic lengths over which the potential, field and current j_y decrease for $|q_y l| \ll 1$ equal

$$\delta_\varphi = \delta_{E_y} = \frac{\pi}{2}\left[|q_y|\left(\ln\frac{2}{|q_y|l} + 1\right)\right]^{-1} + \frac{l}{2\pi}\left(\ln\frac{2}{|q_y|l} + 1\right),$$

$$\delta_{E_x} \equiv \frac{1}{E_x(+0)}\int_0^\infty E_x(x)\,dx = \delta_{j_y} = \frac{\sigma_{xx}}{iq_y\sigma_{xy}} = \frac{l}{\pi}\left(\ln\frac{2}{|q_y|l} + 1\right). \tag{47}$$

The amplitude of the current j_x is a maximum (Fig. 3) at the point $x_m \approx \delta_{E_x} = \delta_{j_y}$.

It is important to note that in strong magnetic fields ($|q_y l| \ll 1$) the EMP is localized near the edge of the system over a length which is small compared to the wavelength $2\pi/|q_y|$ (in contrast to the surface plasmon for a semi-infinite $3D$ plasma). This circumstance validates the rule (13) for quantization of q_y in a sample of finite dimensions if the length (47) is small compared to the transverse dimensions of the $2D$ layer (i.e., in a strong field $\mathbf{B}$).

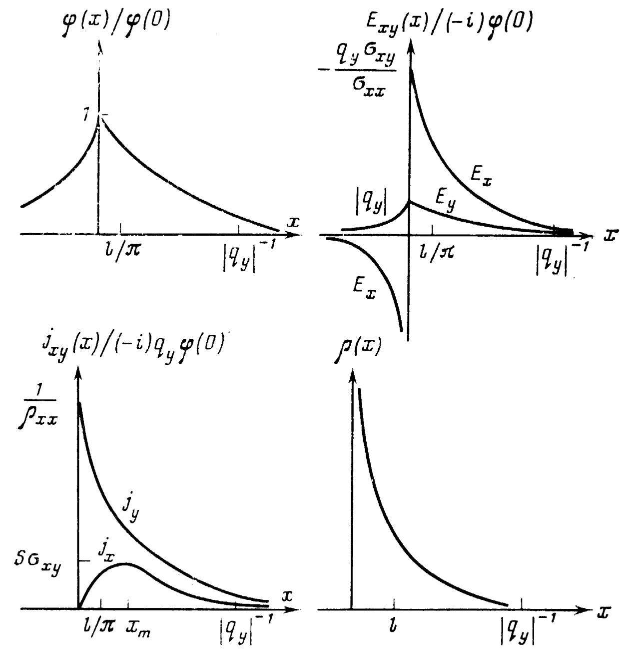

FIG. 3. Amplitude distributions of EMP potential, field, current, and charge density for a $2D$ system at a heterostructure.

The influence of diffusion. In deriving (15) we neglected the diffusion current, which is correct if $|\nabla\varphi| \gg |\nabla p\partial\mu/\partial n_s|/e^2$, where μ is the chemical potential, and $\omega\tau^* \ll 1$. This condition is violated, as follows from (46), when

$$\pi x/|l| \lesssim [\pi a_B N_0/2|l|N(E_F)]^{2}. \tag{48}$$

Here $N(E_F) = \partial n_s/\partial\mu$ is the density of states at the Fermi level. $N_0 = m^*/2\hbar^2$ is the $B = 0$ density of states, $a_B = \hbar^2\tilde{\varkappa}/m^*e^2$ is the Bohr radius. Estimates show that in general the right side of (48) is small. On the one hand, this justifies our neglect of diffusion when calculating the EMP spectrum; on the other hand, it also ensures that the divergence of $\rho_+(x)$ as $x \to +0$ and that of $E_x(x)$ as $x \to -0$ are cut off. By including the smearing-out of the edge ($n_s = n_s(x)$), we also remove the divergence of $\rho_+(x)$ as $x \to +0$ and $E_x(x)$ as $x \to -0$. The corresponding length is the width of the transition layer h.

Influence of the image forces at the lateral boundary. The dispersion relation (37) with the dielectric function (A.1) we will write in the form of (40), where $\tilde{\varkappa} \approx \varkappa^R/2 \gg \varkappa^L$, and in place of F_1 there stands the function

$$F_2(z) = \frac{1}{(1-(z/2)^2)^{1/2}} \ln\frac{1+(1-(z/2)^2)^{1/2}}{z/2}.$$

The EMP spectrum is qualitatively similar to that shown in Fig. 2; however, in contrast to the case $\alpha = 0$ ($\varkappa^R = \varkappa^L$) the EMP branch $\omega_-(q_y)$ and also the edge plasmon branch ($B = 0$) disappear: they are forced down as $\alpha \to 1$ to the lower edge of the ω_{mp} $(0, q_y)$ continuum of $2D$ magnetoplasmons (2). The gapless EMP branch is changed in a insignificant way:

$$\omega_+^2(q_y)\approx\omega_p^2(0,q_y)\,[1-2\omega_c^2/\omega_p^2(0,q_y)],\qquad \omega_c\ll\omega_p(0,q_y),$$

$$\omega_+(q_y)=-\frac{2q_y\sigma_{xy}}{\tilde{\varkappa}}\left[\ln\frac{4}{|q_y|l}+o(1)\right],\qquad |q_yl|\ll 1.$$

EMP at the boundary between two semi-infinite planes. This problem contains two lengths l: an l^L for the left half-plane and an l^R for the right half-plane. The dispersion relation simplifies in the long-wave limit ($|q_y l^L|\ll 1$, $|q_y l^R|\ll 1$):

$$\omega(q_y)=-\frac{2q_y\delta\sigma_{xy}}{\tilde{\varkappa}}\left[\frac{l^R\ln(2/|q_y|l^R)-l^L\ln(2/|q_y|l^L)}{l^R-l^L}+1+o(1)\right].\qquad (49)$$

This equation, just as for (41), is solved by iterations. In particular, the EMP attenuation is small for any $\omega\tau^*$, and for $\omega\tau_R^*\ll 1$, $\omega\tau_L^*\ll 1$ is proportional to $\delta\sigma_{xy}$ and is quantized in the QHE regime:

$$\omega''(q_y)\approx-\pi|q_y(\sigma_{xy}^R-\sigma_{xy}^L)|/\tilde{\varkappa}.$$

A two-dimensional system in the QHE regime with short-range fluctuations of the random potential contains potential regions ("islands" and "hills"), at the edge of which the degree of degeneracy of the Landau levels (and the conductivity) changes discontinuously.[36] Along the perimeter of these regions EMP-like excitations can propagate with the spectrum (49); q_y will take on the discrete values (13), if the corresponding lengths (47) are small compared to the linear dimensions of the region (P is the region's perimeter). If, however, the edge of the region is smeared out by an amount $h>|l^{R,L}|/\pi$, then the EMP spectrum in the region are described by the expression [see (71)]:

$$\omega(q_y)=-\frac{2q_y\delta\sigma_{xy}}{\tilde{\varkappa}}\left[\ln\frac{1}{|q_y|h}+O(1)\right].\qquad (50)$$

The presence of the discrete low-frequency modes (49), (50), and (13) will be manifested in the response of the system in the QHE regime.

Effect of finite substrate thickness. A more realistic situation is one where the semi-infinite $2D$ layer ($x\geqslant 0$) is located at the surface of a dielectric layer (of permittivity $\varkappa$) which occupies the region $0\leqslant z\leqslant d$. Let us analyze Eq. (28) with the dielectric function (A.2); $\sigma_{\alpha\beta}^L=0$, $\sigma_{\alpha\beta}^R\equiv\sigma_{\alpha\beta}$. In the limits $d\to 0$ and $d\to\infty$, (A2) reduces to the case investigated earlier, (A1), if we replace $\tilde{\varkappa}$ by 1 and $\tilde{\varkappa}$ by $(\varkappa+1)/2$, which is physically obvious. The most interesting case is that of a moderately thin substrate: $|l|\ll d\ll|q_y|^{-1}$; here $l=2\pi i\sigma_{xx}/\omega\tilde{\varkappa}$, $\tilde{\varkappa}=(\varkappa+1)/2$. Using the tanh qd approximation

$$\operatorname{th}x\to\min\{x,1\},\qquad (51)$$

in the limit $|q_y l\tilde{\varkappa}|\ll 1$, $\varkappa\gg 1$ we obtain for the gapless EMP branch

$$\omega(q_y)\approx-\frac{2q_y\sigma_{xy}}{\tilde{\varkappa}}\left[\ln\frac{d}{|l|}+\tilde{\varkappa}F_3\left(\frac{\varkappa d|q_y|}{2}\right)\right]$$

$$-i\frac{2|q_y\sigma_{xy}|}{\tilde{\varkappa}}\arg l,\qquad (52)$$

where

$$F_3(z)=(1-z^2)^{-1/2}\ln[(1+(1-z^2)^{1/2})/z].$$

5. EMP FOR THE 2D ELECTRON SYSTEM AT THE SURFACE OF LIQUID HELIUM

Let us investigate the properties of EMP in a system with the dielectric function (A3) and a sharp profile $\sigma_{\alpha\beta}(x)$; $\sigma_{\alpha\beta}^L=0$, $\sigma_{\alpha\beta}^R=\sigma_{\alpha\beta}$.

Edge plasmons ($B=0$). Equation (28) for $B=0$ has a solution in the collisionless approximation

$$\omega^2(q_y)=\omega_p^2(0,q_y)/\eta(|q_yd|)$$
$$=2\pi n_s e^2 q_y\tanh(q_yd)/m^*\tilde{\varkappa}\eta(|q_yd|),\qquad (53)$$

where $\omega_p\ (q_x,q_y)$ is the spectrum of normal $2D$ plasmons in this system, $\eta(z)\approx\eta_0$ for $z\gg 1$ and $\eta(z)\approx 1+(2\ln 2/\pi)^2z^2$ for $z\ll 1$. In the general case $\eta(z)$ is the solution to the equation

$$\int_0^{\pi/2}dx\ln\left[\frac{\eta\tanh(z/\sin x)}{\sin x\tanh z}-1\right]=0.$$

The potential of an edge plasmon (53) decays into the interior of the $2D$ system exponentially for large x with a characteristic length $\pi/(2\ln 2q_y^2d)$ for $|q_yd|\ll 1$, which is far larger than that of a heterostructure. This coincides with the results of Ref. 26.

EM spectrum ($B\neq 0$). For $|q_yd|\gg 1$ the results reduce to those obtained earlier. In the long-wavelength limit, $|q_y|d\ll 1$, $|q_yl|\ll 1$, we can write the dispersion relation in the form (40) by replacing $F_1(|q_y|l)$ by $F_4(l/d)$, where

$$F_4(z)=\frac{1}{z}\int_0^\infty dx\ln\left[1+\frac{z}{x}\tanh\frac{1}{x}\right]$$

$$\approx\begin{cases}\ln\dfrac{1}{z}+A_1+O(z), & |z|\ll 1\\[2mm] \dfrac{\pi}{z^{1/2}}-\dfrac{A_2}{z}+O(z^{-2}), & |z|\gg 1\end{cases},\qquad (54)$$

here $A_1=1+C+\ln(4/\pi)\approx 1.818$, where $C=0.577...$ is Euler's constant and $A_2=2\ln 2\approx 1.386$. For comparison with experiment, it is convenient to use an interpolation formula for F_4:

$$F_4(z)\to\tilde{F}_4(z)=\frac{2}{z^{1/2}}\arctan z^{1/2}+\ln\left(1+\frac{1}{z}\right),$$

which is obtained by using approximation (51).

We obtain the following results for the dependence of the relation between d and $l=l_0+il$, from (54). For large ω ($\omega\tau^*\gg 1$), large B ($l_0\ll d$), and $l_1\ll l_0\ll d$:

$$\omega_+(q_y)\approx-\frac{2q_y\sigma_{xy}}{\tilde{\varkappa}}\ln\frac{(2.71\ldots)^{A_1}d}{l_0}$$

$$-\frac{i}{\tau^*}\left[\ln\frac{(2.71\ldots)^{A_1}d}{l_0}\right]^{-1}.\qquad (55)$$

For small ω ($\omega\tau^* \ll 1$), large B, and $l_0 \ll l_1 \ll d$ [the function f is defined in (43)]:

$$\omega_+(q_y) \approx -\frac{2q_y\sigma_{xy}}{\tilde{\varkappa}} f\left(\frac{(2.71\ldots)^{A_1}d|q_y\sigma_{xy}|}{\pi\sigma_{xx}'}\right) - i\frac{\pi|q_y\sigma_{xy}|}{\tilde{\varkappa}}. \tag{56}$$

For large ω ($\omega\tau^* \gg 1$), small B, and $l_0 \gg \max(l_1, d)$:

$$\omega_+(q_y) \approx -\frac{2\pi q_y\sigma_{xy}}{\tilde{\varkappa}}\left(\frac{d}{l_0}\right)^{1/2}\left[1 - \frac{A_2}{\pi}\left(\frac{d}{l_0}\right)^{1/2}\right]$$
$$-\frac{i}{2\tau^*} = c_p q_y\left[1 - \frac{A_2}{\pi}\frac{d\omega_c}{c_p}\right] - \frac{i}{2\tau}. \tag{57}$$

In the last relation, we have used the Drude model, and $c_p = (2\pi n_s e^2 d/m^*\tilde{\varkappa})^{1/2}$ is the velocity of the "screened" $2D$ plasmon.

In the remaining case, i.e., $l_1 \gg \max(l_0, d)$, the EMP is strongly damped:

$$\omega_+(q_y) \approx -iq_y^2 2\pi d/\rho_{xx}'\tilde{\varkappa}. \tag{58}$$

where $\rho_{xx}' = \sigma_{xx}'/(\sigma_{xx}'^2 + \sigma_{xy}^2)$ is the diagonal resistance. The attenuation time is the product of the resistance of a conducting strip of width $|l|$ and length $|q_y|^{-1}$ $(\rho_{xx}'/|q_y l|)$ and capacitance $\tilde{\varkappa}|l|2\pi d|q_y|$.

Thus, the presence of metallic electrons near the $2D$ layer leads to softening of the EMP frequency for $|q_y d| < 1$ and to the appearance of considerable attenuation for small ω. In a weak field ($l_0 \gg d$) the EMP attenuation is large for $\omega\tau^* < 1$ (as for a normal plasmon), while in a strong field ($l_0 \ll d$) the attenuation is large for $\omega\tau^* \lesssim l_0/d \ll 1$.

Distribution of potential and field for the $\omega_+(q_y)$ EMP mode. The behavior of $\varphi(x)$ as $x \to 0$ is determined by the asymptotic form of $\varepsilon(q_x)$ as $q_x \to \infty$, which is the same for all $2D$ systems, i.e., (A1)–(A5). Therefore $\varphi_\pm(x), \rho_\pm(x)$ are described by the expressions (46) for $|x| \ll |l|$, d and $|q_y|^{-1} \gg |l|, d$.

The behavior of $\varphi(x)$ for $x > 0$ is determined by the simple zeroes

$$q_x = -i\alpha_n = -i\left(q_y^2 + \left[\frac{\pi\gamma_n(d/l)}{d}\right]^2\right)^{1/2}, \quad n = 1, 2, \ldots$$

of the function $\varepsilon(q_x)$ see (A3) in the lower half-plane (the $\gamma_n(x)$ are roots of the equation $\tan(\pi\gamma_n) = x/(\pi\gamma_n)$), while for $x < 0$ it is determined by the simple poles

$$q_x = i\beta_n = i\left(q_y^2 + \left(\frac{\pi(n - 1/2)}{d}\right)^2\right)^{1/2}, \quad n = 1, 2, \ldots$$

of the function $\varepsilon(q_x)$ in the upper q_x half-plane [in contrast to (A1), there are no branch points in (A3)]. The asymptotic form of $\varphi(x)$ as $|x| \to \infty$ is determined by the singularity of $\varepsilon(q_x)$ which is closest to the real axis. For $|q_y|d \ll 1$, $|q_y|l \ll 1$, in a strong magnetic field (i.e., $|l| \ll d$), when (55), (56) are applicable, then $\alpha_1 \approx \beta_1 \approx \pi/2d$ and

$$\varphi_\pm(x) \approx -\varphi(0)\frac{4q_y\sigma_{xy}}{\omega\tilde{\varkappa}} X_\mp\left(\mp\frac{i\pi}{2d}\right)\exp\left(\mp\frac{\pi x}{2d}\right), \quad |x| > \frac{d}{\pi}; \tag{59}$$

in a weak magnetic field (i.e., $l_0 \gg l_1, d$) under conditions such that (57) is applicable, $\alpha_1 \approx (dl_0)^{-1/2}$, $\beta_1 \approx \pi/2d$ and

$$\varphi_+(x)|_{x > d/\pi} \approx \varphi(0)\exp(-x/(dl_0)^{1/2}),$$
$$\varphi_-(x)|_{x < -2d/\pi} \approx \frac{2\varphi(0)}{\pi}\exp\left(\frac{\pi x}{2d}\right). \tag{60}$$

The local capacitance approximation. Equation (60) for $\varphi_+(x)$ satisfies the boundary condition $j_x(+0) = 0$ [see (31)], and therefore is applicable not only for $x > d/\pi$, but also for all $x > 0$. It was obtained as $d \to 0$ ($d \ll |l|$, $|q_y|^{-1}$, to be more precise). In the limit $d \to 0$ the kernel of Eq. (15) becomes a δ-function ($G_{qy}(x; 0, 0) \to d\delta(x)/2\tilde{\varkappa}$); (15) reduces to the equation for a parallel-plate capacitor $\rho(x)/\varphi(x) = \tilde{\varkappa}/2\pi d$, and the EMP problem reduces to solution of an ordinary second-order differential equation with the boundary condition $j_x(+0) = 0$. This local-capacitance approximation is often used in calculating the dynamic properties of $2D$ systems with metallic electrodes (one or two)[9,26,37]; its applicability requires not only the condition $|q_y|d \ll 1$, but also the stricter inequality $d \ll |l|$. A part of the information is lost when this approach is taken, e.g., the singularity in $\rho_+(x \to 0)$ is not described.

6. EMP IN METAL-INSULATOR-SEMICONDUCTOR STRUCTURES

Let us analyze the EMP spectrum in a MIS structure with the dielectric function (A4). For $|q_y|d \gg 1$ the results reduce to those obtained earlier. We denote the ratio $\varkappa_2/\varkappa_1$ by β. Let us write the dispersion relation in the small-q_y limit ($|q_y|^{-1} \gg d, \beta d, |l|$) in the form (40), replacing F_1 with $F_5(l/d)$:

$$F_5(z) = \int_0^\infty dx \ln\left[1 + \frac{1+\beta}{x(\beta + \coth(1/xz))}\right]$$

$$\approx \begin{cases} \ln\frac{1}{z} + 1 + g(\beta) + o(1), & |z| \ll 1 \\ \pi((1+\beta)/z)^{1/2}, & |z| \gg 1 \end{cases}, \tag{61}$$

$$g(\beta) = \int_0^\infty \frac{(1+\beta)\ln(1/x)dx}{(\cosh x + \beta\sinh x)^2}. \tag{62}$$

The function $g(\beta)$ possesses the following properties: $g(0) = C + \ln(4/\pi) \approx 0.819$, $g(1) = C + \ln 2 \approx 1.270$, $g(\beta) \approx \ln\beta + \beta^{-1}(\ln\beta + 0.568)$ as $\beta \to \infty$. With the help of (51), we obtain the interpolation formula

$$g(\beta) \to \beta^{-1}(1+\beta)\ln(1+\beta).$$

We now present a summary of the results for the spectrum of the gapless EMP mode in the long-wavelength limit:

$$\omega_+(q_y) \approx -\frac{2q_y\sigma_{xy}}{\tilde{\varkappa}}\left[\ln\frac{d}{l_0} + 1 + g(\beta)\right]$$
$$+\frac{i}{\tau^*}\left[\ln\frac{d}{l_0} + 1 + g(\beta)\right]^{-1}, \quad l_1 \ll l_0 \ll d,$$

$$\omega_+(q_y) \approx -\frac{2q_y\sigma_{xy}}{\tilde{\varkappa}} f\left(\frac{d|q_y\sigma_{xy}|}{\pi\sigma_{xx}'}\exp[1 + g(\beta)]\right)$$

$$-i\frac{\pi|q_y\sigma_{xy}|}{\tilde{\varkappa}}, \quad l_0\ll l_1\ll d,$$

$$\omega_+(q_y)\approx-\frac{2q_y\sigma_{xy}}{\tilde{\varkappa}}\pi\left(\frac{d}{l_0}(1+\beta)\right)^{1/2}-\frac{i}{2\tau^*}, \quad l_0\gg l_1, d.$$

For $l_1\gg l_0$, d the EMP is strongly damped. The asymptotic form of $\varphi_+(x)$ as $x\to\infty$ has contributions both of the form (46) determined by the branch point of the function $\varepsilon(q_x)$ and of the form (59), (60) determined by the screening effect of the metallic electrode.

7. PROBLEMS WHICH CAN BE SOLVED BY APPROXIMATE METHODS

The Wiener-Hopf method cannot be applied to find the properties of EMP in a $2D$ structure of complicated geometry; therefore it becomes necessary to perform the analysis by approximate methods. The simplest of these methods—the local capacitance method—is applicable only in structures with metallic electrodes and only in sufficiently small fields **B** ($d\ll|l|$, $|q_y|^{-1}$).

Let us investigate another approximate method which is suitable for strong magnetic fields, when the width of the region in which the EMP is localized is smaller than the remaining lengths of the problem. In this case, for a heterostructure with a sharp profile (see Appendix 4)

$$\varphi(x)\approx-\varphi(0)\frac{4\pi q_y\sigma_{xy}}{\omega}G_{q_y}(x;0,0), \quad x\gg|l|/\pi. \quad (63)$$

Near the edge of the $2D$ system the asymptotic form (A12) is valid; from (63) and (A12) it follows that $\varphi_+(x)\approx\varphi(0)$ at least for $x\ll|lS|/\pi$. For $|S|\gg1$ the region of applicability of the latter equation and (63) overlap. Therefore, setting $x=\gamma_0 l$ $(1\ll\pi\gamma_0\ll S)$ in (63) and cancelling the factor $\varphi(0)\approx\varphi(\gamma_0 l)$, we obtain the dispersion relation for S,

$$S\approx\ln\frac{1}{|q_y|l}+A_3+o(1), \quad |q_y l|\ll1,$$

which coincides to logarithmic accuracy ($|S|\gg1$) with the exact form (41). The constant $A_3=\ln(2/\gamma_0)-C$ remains undetermined using this approach. The value $\gamma_0=\gamma=\exp(-1-C)\approx0.207$ corresponds formally to the exact value $A_3=\ln 2+1$ which follows from (41). Let us apply this approach to the solution of the EMP problem for samples with the shape of a strip or disk.

EMP in a strip of finite width. Let us investigate a system with the dielectric function (A1) in a strip

$$-L_x/2\leqslant x\leqslant L_x/2, \quad -\infty<y<+\infty, \quad z=0.$$

For $|x\mp L_x/2|\gg|l|/\pi$, we obtain in analogy with (63)

$$\varphi(x)=\frac{2q_y\sigma_{xy}}{\omega\tilde{\varkappa}}\left\{\varphi\left(\frac{L_x}{2}\right)K_0\left(|q_y|\left|x-\frac{L_x}{2}\right|\right)-\varphi\left(-\frac{L_x}{2}\right)K_0\left(|q_y|\left|x+\frac{L_x}{2}\right|\right)\right\}. \quad (64)$$

After substituting $x=\pm(L_x/2-\gamma_0 l)$ for

$$|\gamma_0 l|\ll L_x, \quad \varphi(\pm L_x/2)\approx\varphi(\pm L_x/2\mp\gamma_0 l)$$

we have an eigenvalue problem; from these eigenvalues we find two EMP branches:

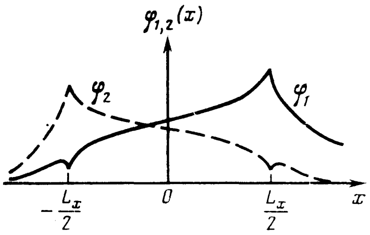

FIG. 4. Amplitude distributions of EMP potential for the two gapless branches in the strip $-L_x\leqslant x\leqslant L_x$, $-\infty<y<\infty$.

$$\omega_{1,2}(q_y)\approx\pm\frac{2q_y\sigma_{xy}}{\tilde{\varkappa}}[K_0^2(\gamma_0|q_y|l)-K_0^2(|q_y|L_x)]^{1/2}. \quad (65)$$

Corresponding to branch ω_2 (ω_1) there is an EMP traveling along (opposite to) the y-axis and localized primarily near the left (right) edge of the strip (see Fig. 4). As $L_x\to\infty$ $L_x\gg\delta_{E_x}=\pi^{-1}\, l\ln(5.4/|q_y|l$ to be more precise), both branches (65) reduce to (41) if $\gamma_0=\gamma=0.207$. For $L_x\ll|q_y|^{-1}$ the dependence of the EMP frequency on wave vector is similar to the spectrum of a 10 plasmon ($\omega^2\propto q^2\ln(1/q)$):

$$\omega_{1,2}(q_y)\approx\pm\frac{2q_y\sigma_{xy}}{\tilde{\varkappa}}\left[2\ln\frac{L_x}{\gamma l}\ln\frac{5.436\gamma^{1/2}}{|q_y|(L_xl)^{1/2}}\right]^{1/2}. \quad (66)$$

The attenuation of the EMP in cases (65), (66) is small ($\omega''\ll\omega'$); however, for very small ω, when $|l|\approx l_1=2\pi\sigma'_{xx}/\omega\tilde{\varkappa}$ is comparable to L_x, the solution (64) is inapplicable and the EMP begins to be strongly damped. In the QHE regime $\sigma'_{xx}(0)$ is very small and the EMP is weakly damped for $\omega/2\pi\gg\sigma'_{xx}/\tilde{\varkappa}L_x\sim1$ Hz, if $\sigma'_{xx}\sim10^{-12}\Omega^{-1}$, $L_x\sim1$ cm, and $\tilde{\varkappa}\sim1$.

2D disk in an external field. Let us investigate the response of the $2D$ layer having the form of a disk of radius R and the dielectric function (A1) in an AC electric field of frequency ω lying in the plane of the disk. The first of Eqs. (15) now determines the potential $\varphi_{\rm ind}$ induced by the external potential $\varphi_{\rm tot}=\varphi_{\rm ext}+\varphi_{\rm ind}$. In cylindrical coordinates

$$\varphi(r,\theta,z=0)=\sum_n\varphi^n(r)\exp(in\theta)$$

for $|l|/\pi\ll R$ and $R-r\gg|l|/\pi$ we obtain for $\varphi^n(x)$

$$\varphi^n_{ind}(r)=\frac{2n\sigma_{xy}}{\omega\tilde{\varkappa}R}\varphi^n_{tot}(R)\int_0^\pi\frac{d\theta\cos n\theta}{[1-(2r/R)\cos\theta+(r/R)^2]^{1/2}} \quad (67)$$

where $n=\pm1,\pm2,\ldots$. After we set $r=R-\gamma_0 l$ in the integral (which we denote by I_n) and assume $\varphi^n_{\rm ind}(R)\approx\varphi^n_{\rm ind}(R-\gamma_0 l)$, we express $\varphi^n_{\rm tot}$ in terms of $\varphi^n_{\rm ext}$:

$$\varphi^n_{tot}(R)=\varphi^n_{ext}(R)/\tilde{\varepsilon}(n,\omega), \quad (68)$$

$$\varphi^n_{tot}(r)\approx\varphi^n_{ext}(r)+\frac{\omega_+(n)}{\omega}\varphi^n_{tot}(R)\frac{I_n(r/R)}{I_n(1-\gamma_0 l/R)},$$

$$|r-R|\gg|l|/\pi.$$

The quantity $\tilde{\varepsilon}(n,\omega)=1-\omega+(n)/\omega$ is in some sense the dielectric function of the disk, and vanishes at the EMP frequency

$$\omega_+(n) \approx \frac{2n\sigma_{xy}}{\tilde{\varkappa}R} I_n\left(1-\gamma_0\frac{l}{R}\right).$$

After estimating I_n for $|\gamma_0 l/R| \ll 1$ and using the value $\gamma_0 = \gamma = 0.207$ for γ_0 (in this case (69) reduces to (41) in the limiting case of the half-plane, i.e., $R\to\infty$, $n\to\infty$, $q_y = -2\pi n/P = -n/R = \text{const.}$), we find the spectrum of discrete EMP modes of the disk

$$\omega_+(n) = \frac{2n\sigma_{xy}}{\tilde{\varkappa}R}\left\{\ln\frac{2R}{l} - \Psi\left(|n| + \frac{1}{2}\right) + 1 + o(1)\right\}, \quad (69)$$

where Ψ is the digamma function. We note that (69) is very close to (41), (13) not only for $n\to\infty$ but also for $n = 1$. This is still another confirmation of the applicability of condition (13) for $|l/\pi| \ll R$ for finite-dimensional samples. The response to the real harmonic $\varphi^n_{\rm ext}(r)$ is obtained by adding $\varphi^n_{\rm tot}$ and $\varphi^{-n}_{\rm tot}$, taking into account that $\omega_+(-n) = -\omega_+^*(n)$.

Effect of a profile in $\sigma_{\alpha\beta}(x)$. In real $2D$ systems the $2D$ electron concentration $n_s(x)$ near the boundary varies smoothly over a length h. It is necessary to include this, especially for electron systems at the surface of helium, in which h is on the order of the distance to the metallic electrodes d.[9,26] For $|l| \gg h$ the effect of smearing out this boundary is small and the theory of Sec. 3 is valid. In a strong magnetic field, the role of the transition layer becomes important when $|l| \lesssim h$. Let us investigate the EMP spectrum of a semi-infinite $2D$ layer with a smeared-out edge in a strong field $\mathbf{B}$ in the long-wavelength limit. The transition layer will be described by a function $\tilde{\theta}(x/h)$ (see Appendix 4). For $|lS|/\pi \ll h,d$ the following equation is implied by (15) and (A14):

$$\varphi(x) \approx -\frac{4\pi q_y\sigma_{xy}}{\omega}\int_{-\infty}^{+\infty} dx' G_{q_y}(x-x';0,0)\varphi(x')\frac{\partial\tilde{\theta}(x'/h)}{\partial x'}. \quad (70)$$

Let us first investigate the case of a heterostructure (i.e., $G_{q_y}(x-x';0,0) = K_0(|q_y||x-x'|)/2\pi\tilde{\varkappa}$). When the potential φ varies smoothly over the length h, we can evaluate it at the point $x' = 0$ and take it outside the integral (it is easy to verify that this is permissible when $|q_y|h \ll 1$). We then set $x = 0$, cancel the $\varphi(0)$ factors, and obtain

$$\omega_+(q_y) \approx -\frac{2q_y\sigma_{xy}}{\tilde{\varkappa}}\int_{-\infty}^{+\infty} d\xi K_0(|q_y h\xi|)\frac{\partial\tilde{\theta}(\xi)}{\partial\xi}.$$

Expanding the integral for $|q_y|h \ll 1$ gives

$$\omega_+(q_y) = -\frac{2q_y\sigma_{xy}}{\tilde{\varkappa}}\left[\ln\frac{2}{|q_y|h} - C + A_4\right]. \quad (71)$$

The value of the constant A_4 depends on the explicit form of $\tilde{\theta}(x/h)$:

$$A_4 = \int_{-\infty}^{\infty} d\xi \ln\frac{1}{|\xi|}\frac{\partial\tilde{\theta}(\xi)}{\partial\xi}.$$

For the electron system at the surface of liquid helium, the condition $|q_y|d \ll 1$ implies

$$G_{q_y}(x-x';0,0) = \ln \operatorname{cth}[\pi|x-x'|/4d]/2\pi\tilde{\varkappa}.$$

Substituting $x = d\xi$, $x' = d\xi'$ into (70), we obtain

$$\varphi(\xi d) = \frac{1}{S}\int_{-\infty}^{+\infty} d\xi' \ln\coth\left(\frac{\pi}{4}|\xi-\xi'|\right)\varphi(\xi' d)\frac{\partial\tilde{\theta}(d\xi'/h)}{\partial\xi'}. \quad (72)$$

From this it follows that $S = -\omega\tilde{\varkappa}/2q_y\sigma_{xy}$ is a function of the ratio h/d:

$$\omega_+(q_y) = -\frac{2q_y\sigma_{xy}}{\tilde{\varkappa}}F_6(h/d). \quad (73)$$

In order to calculate $F_6(x)$ it is necessary to solve the complicated integral equation (72). However, in the case of a weakly smeared-out profile ($h \ll d$), after solving (72) by using the same method as for the heterostructure, we obtain an estimate for the EMP frequency:

$$\omega_+(q_y) = -\frac{2q_y\sigma_{xy}}{\tilde{\varkappa}}\left[\ln\frac{4d}{\pi h} + A_4\right]. \quad (74)$$

Comparing (71) with (41) and (74) with (54), we can conclude that in systems with weakly smeared-out edges and in the case where $|l|$ is smaller than all the remaining lengths in the problem, the effect of the profile $n_s(x)$ reduces to replacing l by h. This implies that in such systems the EMP charge is localized in a strip whose width is of order $b = \max(|l|, h)$ (compare with (A14) and Sec. 2).

8. DISCUSSION OF RESULTS AND COMPARISON WITH EXPERIMENT

In an inhomogeneous $2D$ electron gas collective excitations can thus propagate along a line separating regions of differing conductivity (in particular, along the boundary of the $2D$ system); the appearance of these excitations (called edge plasmons and magnetoplasmons) is connected with the loss of translation invariance. In a strong $\mathbf{B}$ field their frequencies can be considerably less than ω_c; the direction of their propagation is given by the vector $[\nabla n_s(\mathbf{r}), e\mathbf{B}]$.

EMP also have the following quantum interpretation.[11] It takes an energy $\hbar\omega_c$ to create a single-particle excitation in an infinite sample, which leads to the gap ω_p in the magnetoplasmon spectrum (2). The presence of a boundary in the $2D$ system gives rise to a kink in the Landau levels and to the appearance of Fermi points (i.e., points in the space of centers of the Landau oscillators at which the Fermi level intersects a Landau level); that is, the system acquires the properties of a low-dimensional metal. This means that the presence of gapless boundary electronic states at the Fermi level, which correspond to electrons "hopping" along the edge, gives rise to the appearance of gapless (or, in finite samples, low-frequency) EMP. The direction of their motion coincides with the direction along which the electrons "hop". When N Landau levels are occupied there are N Fermi-points in a semiinfinite sample. The EMP correspond to in-phase oscillations of electrons at all these points. In addition, for $N > 1$ there are also $N - 1$ branches of lower-frequency excitations with acoustic spectra. These correspond to out-of-phase oscillations of the Fermi electrons (in Ref. 11, these are called acoustic EMP). These excitations have not yet been seen in experiments.

Let us compare the EMP in a $2D$ system with the analogous modes in the $3D$ case—the surface magnetoplasmons.

The primary difference in the $2D$ case is the presence in the problem, along with the wavelength $2\pi/|q_y|$, of (at least) one other complex length $l(\omega, B)$, which determines the spatial dispersion of the dielectric permittivity (in the simplest case, $\varepsilon(\mathbf{q}, \omega) = 1 + ql$). Including the latter in the $2D$-case has a fundamental effect. On the one hand, this strongly complicates the problem, while on the other hand it leads to nontrivial features in the EMP. In particular, the EMP in a strong **B** field is localized much more strongly compared to the $3D$ case over lengths which are small compared to the wavelength.

The first time that EMP were actually detected experimentally to our knowledge was in Ref. 8, during the investigation of IR light absorption in a GaAs–AlGaAs heterostructure consisting of a set of disks with diameter $2R = 3$ μm. As **B** was increased, there appeared a splitting of the resonance frequency of the type shown in Fig. 2b. Comparison of the theory (69) with experiment[8] using the framework of the Drude model (this is possible for the three points which have $\omega < \omega_c$, see Fig. 4 in Ref. 8, and which lie in the region of applicability of (69) since for them $|l|/\pi R \lesssim 0.1$) gives agreement to an accuracy of better than 10%, where the accuracy is determined by the size of the points on Fig. 4 of Ref. 8. In Refs. 23–25 the fundamental EMP mode is investigated at radio and microwave frequencies ($P \approx 1$ cm) for heterostructures in the QHE regime. For the low-mobility electron gas in Ref. 24 the condition $\omega\tau^* < 1$ holds, and the functions $\omega'(B)$ and $\omega''(B)$ are in qualitative agreement with Eq. (43). For a quantitative comparison it is necessary to include the real geometry of the dielectric substrate. In samples with high-mobility electrons[23,25] it is clear that the condition $\omega\tau^* > 1$ holds. A comparison of (42), (13) with the data from Refs. 23, 25 allows us to obtain a reasonable order-of-magnitude estimate of the parameters of the theory: $\tau^* \sim \tilde{\varkappa}^{-1} \cdot 10^{-8}$ sec. $\omega'\tau^* \sim 12/\tilde{\varkappa}$, $|q_y l| < 10^{-3}$ for an occupation of $\nu = 2$; here $\tilde{\varkappa} \sim 1$ (see the discussion in Ref. 24).[2]

In Ref. 8 a theory was formulated to explain the results of experiments on the basis of the effect of the depolarizing field which arises in a $2D$ disk, where the latter was modeled as an oblate conducting (Drude model) ellipsoid. Independently, a similar approach was used in Refs. 13, 25, and 27 for calculating the frequency[13] and attenuation[25] of characteristic oscillations of such a disk (in Ref. 27 the system was a superlattice in the shape of an ellipsoid) in a strong magnetic field ($\sigma_{xx}/\sigma_{xy} = 0$). Among other peculiarities of the ellipsoid model we should mention the strong inhomogeneity of the concentration $n_s(r)$ (Ref. 22) of $2D$ electrons (and consequently of $\sigma_{xy}(r)$), and the homogeneity of the field for $n = 1$. For the low-frequency branch ($\omega \ll \omega_c$) this approach gives (for $n = 1$):

$$\omega' = {}^3/_4\pi^2\sigma_{xy}/R\tilde{\varkappa}, \quad \omega'' = {}^3/_4\pi^2\sigma_{xx}'/R\tilde{\varkappa} \tag{75}$$

[the results obtained in Refs. 8, 13, and 25 differ from (75) by a numerical factor which was introduced in Ref. 22]. From this it is clear that the results of calculating the EMP frequency ω' in the ellipsoidal model differ from (42), (43) by a factor which is weakly (i.e., logarithmically) dependent on the parameters of the problem, while the differences in the EMP attenuation ω'' calculated from (75) and (42), (43) can be very important, especially in the QHE regime where $\sigma_{xx}' \to 0$. In the experiments[8,23,25] the values of q_y, n_s and B do not vary over a very large range; therefore, Eq. (75) for ω' should agree rather well with experiment. However, measurements of the EMP attenuation show that Eq. (75) gives much too low a value for ω'' (several orders of magnitude for $\nu = 2$).

Thus, the ellipsoidal model cannot be applied to a real $2D$ system with a homogeneous concentration of electrons in a strong magnetic field ($|l| \ll R$). Apparently, this approach can claim to explain the experiments only in the weak magnetic field regime, when $|l| \gtrsim R$ and the localization length of the EMP field is of order $|q_y|^{-1} \sim R$.

The most complete experimental data has been obtained for the $2D$ system at the surface of liquid helium[7,9,18] with metallic electrodes in the form of a rectangle[7] or a disk of radius R[9,18]. Let us investigate the experimental points which lie in the region $|q_y|d \ll 1$, $|q_y l| \ll 1$; here, $q_y = 2\pi n/P$. In a narrow interval of magnetic field, i.e., when $d - h \ll |l| \approx l_0 \ll R/n$, the experimental data[9,18] are described satisfactorily by Eq. (5), which gives corrections to the result $\omega_+ = c_p q_y$ first obtained by the authors of Ref. 9 in the collisionless limit by using the local capacitance approximation.

The strong magnetic field region ($|l| \ll h \sim d$), in which Eq. (73) holds, was investigated in Refs. 7, 18. In this case we have $\omega \propto B^{-1}$. From the slope of the line $\omega(B^{-1})$ as $B^{-1} \to 0$ (see Fig. 2 in Ref. 18) and from comparing with (73), we obtain $F_6(h/d) \approx 2.9$; the radius of the $2D$ disk $R = 0.83$ cm was obtained by comparing the measured (Ref. 18, Fig. 1) and calculated[9] values of the resonance frequency for $B = 0$. A summary given in Ref. 7 of data obtained in a strong magnetic field (see Fig. 2 of Ref. 11) demonstrates that $\omega B/n_s$ is directly proportional to the mode index $n = q_y P/2\pi$. Unfortunately, there was no data given in Ref. 7 which would allow us to determine unambiguously the index of the excited EMP modes. Therefore, there are two possible ways to understand and fit the experimental data. If we assume (see Ref. 11) that the lower excited mode in Ref. 7 corresponds to $n = 2$, while the size of the region occupied by the $2D$ electron gas equalled the size of the metallic electrodes (1.78×2.5 cm^2, $P = 8.56$ cm), then from comparison of the slope of the straight line on Fig. 2 on Ref. 11 with Eq. (73) we obtain $F_6(h/d) \approx 1.25$. If, however, we assume that in Ref. 7 EMP modes are excited starting with $n = 1$, then we obtain a value of $F_6(h/d) \approx 2.5$ which is closer to the results derived in Ref. 18. We remark that in reality the perimeter P of the $2D$ system in Ref. 7 can exceed the value $P = 8.56$ cm used above, because of the specific (see Ref. 38) position of the guard electrode in Ref. 7. This circumstance may possibly explain the discrepancy in the values of $F_6(h/d)$ derived in Refs. 7, 18.

The anomalously small EMP attenuation measured in Ref. 7 agrees qualitatively with the results obtained in Sec. 5.

The authors of Ref. 7 also formulated a theory of EMP based on a solution to an integral equation of type (16) in which the logarithmically divergent kernel was approximated by a simpler (exponential) kernel (see also Ref. 10). Although the authors of Ref. 7 were able to reconcile the theory with experiment by using fitting parameters, their incorrect dependence of $\omega(q_y)$ (which is $\propto q_y^2$ in place of $\propto q_y$ under the experimental conditions of Ref. 7) casts into doubt the correctness of this method. A similar approximation gives an expression (see Ref. 12) for the EMP spectrum of a heterostructure which agrees with (75) in strong magnetic fields with an accuracy up to a coefficient. In Refs. 14, 15 the integral equation was solved numerically (an analogous method for superlattices was used in Refs. 19–21). However, several results of the numerical calculation contain qualitatively nontrivial conclusions. For example, a confirmation[14] of the possible presence of a considerable contribution from a δ-function-like EMP charge at $x=0$ would contradict the finiteness of the field energy of the EMP at the boundary.[29]

To summarize, we can state that the principal deficiency of the modeling calculations of Refs. 7, 8, 10, 12, 13, and 25 is the neglect of the length l which figures into the exact formulation of the problem, which is characteristic of the $2D$ electronic system, and which plays an important role in the formation of the spectrum, potential, and field distribution of the EMP.

The authors are grateful to V. B. Sandomirski, and also to L. A. Galenkov, S. S. Nazin and V. B. Shikin for numerous discussions, and to A. V. Chaplik for useful comments.

APPENDIX 1

The dielectric function of a $2D$ system $\varepsilon(\mathbf{q},\omega)$ is defined by Eq. (18); its explicit form depends on the form of $G(q_x, q_y)$ and on $q=(q_x^2+q_y^2)^{1/2}$. After solving the electrostatic problem for a layered system with dielectric permittivity

$$\varkappa(z)=\begin{cases}\varkappa_0, & z>d_1,\quad z<-d_2\\ \varkappa_1, & 0<z<d_1\\ \varkappa_2, & -d_2<z<0\end{cases}$$

and a $2D$ layer in the plane $z=0$, we obtain

$$\varepsilon(\mathbf{q},\omega)=1+\frac{2\pi i\sigma_{xx}(\omega)}{\omega}\frac{q}{\Delta(q)},$$

$$\Delta(q)=\frac{1}{2}\left\{\varkappa_1\frac{\varkappa_1\tanh qd_1+\varkappa_0}{\varkappa_1+\varkappa_0\tanh qd_1}+\varkappa_2\frac{\varkappa_2\tanh qd_2+\varkappa_0}{\varkappa_2+\varkappa_0\tanh qd_2}\right\}.$$

Using this expression, we obtain for the $2D$ layer at the boundary of two semiinfinite dielectrics $(d_1=d_2=\infty)$, which is typical of modulation-doped heterostructures $(\tilde{\varkappa}=(\varkappa_1+\varkappa_2)/2)$;

$$\varepsilon(q,\ \omega)=1+2\pi i\sigma_{xx}(\omega)q/\omega\tilde{\varkappa}. \tag{A1}$$

A more realistic model of a heterostructure includes the finite thickness of the dielectric substrate $(d_1=0,\ d_2=d,\ \varkappa_0=1,\ \varkappa_2=\varkappa)$:

$$\varepsilon(q,\omega)=1+\frac{2\pi i\sigma_{xx}(\omega)}{\omega}\frac{2q}{1+\varkappa\,(\varkappa\tanh gd+1)/(\varkappa+\tanh qd)}. \tag{A2}$$

For electrons at the surface of liquid helium a metal $(\varkappa_0=\infty)$–dielectric 1–dielectric 2–metal structure is typical, with $d_1=d_2=d$:

$$\varepsilon(q,\omega)=1+\frac{2\pi i\sigma_{xx}(\omega)}{\omega\tilde{\varkappa}}\,q\tanh qd. \tag{A3}$$

In a MIS structure $(\varkappa_0=\infty,\ d_1=d,\ d_2=\infty)$

$$\varepsilon(q,\omega)=1+\frac{2\pi i\sigma_{xx}(\omega)}{\omega}q\frac{2}{\varkappa_1\coth qd+\varkappa_2} \tag{A4}$$

For a superlattice (i.e., a set of $2D$ layers located at $z_n=na$ in a dielectric $(\varkappa)$, where a is the superlattice period and $n=\pm1,\ \pm2,\ldots$)

$$\varepsilon(q,q_z,\omega)=1+\frac{2\pi i\sigma_{xx}(\omega)}{\varkappa\omega}\frac{q\sinh qa}{\cosh qa-\cos q_z a}. \tag{A5}$$

APPENDIX 2

We list here several properties of the functions $X_\pm(q_x)$, which are proportional to the Fourier components of the charge densities $\rho_\pm(x)$. From the definition (19) it follows that

$$X_+(q_x)X_-(-q_x)=1. \tag{A6}$$

After casting (19) in the form of a principal-value integral

$$X_\pm(q_x)=\left[\frac{\varepsilon^R(q_x)}{\varepsilon^L(q_x)}\right]^{\mp1/2}\exp\left\{-\frac{1}{2\pi i}\int_{-\infty}^{\infty}\frac{dq_x'}{q_x'-q_x}\ln\left[\frac{\varepsilon^R(q_x')}{\varepsilon^L(q_x')}\right]\right\},$$

we find the asymptotic form of $X_\pm(q_x)$

$$X_\pm(0)=[\varepsilon^R(0)/\varepsilon^L(0)]^{\mp1/2},\quad X_\pm(q_x\to\infty)\sim[\varepsilon^R(q_x)/\varepsilon^L(q_x)]^{\mp1/2} \tag{A7}$$

Using (A1)–(A5), we obtain for the case $\sigma_{xx}^L,\sigma_{xx}^R\neq0$

$$X_\pm(q_x\to\infty)\sim[\sigma_{xx}{}^R(\omega)/\sigma_{xx}{}^L(\omega)]^{\mp1/2}, \tag{A8}$$

and in the case $\sigma_{xx}^L=0,\ \sigma_{xx}^R\neq0$,

$$X_\pm(q_x\to\infty)\sim\left[\frac{2\pi i\sigma_{xx}{}^R(\omega)}{\omega\tilde{\varkappa}}\,|q_x|\right]^{\mp1/2}. \tag{A9}$$

APPENDIX 3

Let us use the function $F_1(z)$ defined in (40). In the region $\omega^2<\omega_{mp}^2(0,q_y)$, in which the EMP can exist, the parameter z varies in the intervals $(-\infty,-1)$ and $(0,+\infty)$. The integral appearing in $F_1(z)$ can be expressed[39] in terms of a special function—Clausen's integral,[40] whose asymptotic form is given by $(G=0.916\ldots,\ \eta_0=1.217\ldots)$:

$$F_1\approx\ln\frac{2}{z}+1,\qquad |z|\ll1;$$

$$F_1\approx\frac{\pi^2(\eta_0{}^2-1)^{1/2}}{(z+\eta_0)\eta_0[\pi-\arccos(1/\eta_0)]},\qquad |z+\eta_0|\ll1;$$

$$F_1\approx\frac{\pi}{z}\left(1-\frac{1}{z}\right),\qquad |z|\gg1;$$

$$F_1\approx\pi\coth\frac{2G}{\pi}+\frac{\pi(2(-z-1))^{1/2}}{\sinh^2(G/\pi)},\qquad |z+1|\ll1.$$

A graph of $F_1(z)$ is shown in Fig. 5. The singularity of F_1 for $z=-\eta_0$ describes the edge plasmon (39). The regions $(-\infty,-\eta_0)$ and $(0,+\infty)$ correspond to the branch

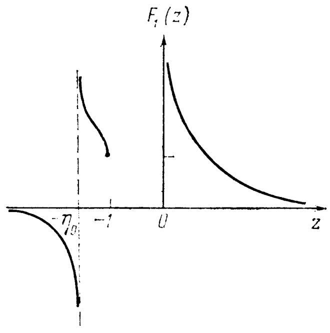

FIG. 5.

$\omega_+(q_y)$, the region $(-\eta_0, -1)$ to the branch $\omega-(q_y)$, the region $(-1, 0)$ to the $2D$ plasmon continuum (2) (here $\operatorname{Im} F_1(z) \neq 0$, which corresponds to collisionless attenuation of the EMP due to decay into $2D$ magnetoplasmons).

APPENDIX 4

Let us investigate the behavior of $\varphi(x)$, $\rho(x)$ in the limits $|q_y l| \ll 1$, $|q_y| h \ll 1$. The transition layer will be described by a smooth function $\tilde{\theta}(x/h)$, which varies from 0 to 1 in the interval $|x| \lesssim h/2$. The charge density $\rho(x)$ [see (15)] we will write in the form of a sum of $\rho_1+\rho_2+\rho_3+\rho_4$:

$$\rho(x)=\frac{\varkappa}{2}\left\{\frac{l}{\pi}\tilde{\theta}\frac{\partial^2\varphi}{\partial x^2}+\frac{l}{\pi}\frac{\partial\tilde{\theta}}{\partial x}\frac{\partial\varphi}{\partial x}-\frac{l}{\pi}q_y{}^2\tilde{\theta}\varphi+\frac{1}{S}\frac{\partial\tilde{\theta}}{\partial x}\varphi\right\}. \tag{A10}$$

For large x, (15) implies a multipole expansion of the potential

$$\varphi(x)=4\pi Q G_{q_y}(x)-4\pi D\frac{\partial G_{q_y}(x)}{\partial x}+\ldots, \tag{A11}$$

where Q and D are the linear charge density and dipole moment of the EMP.

Let us first investigate the case of a heterostructure with a sharp profile ($h=0$). From the requirement that the δ-function-like contribution vanish ($\rho_2+\rho_4=0$, i.e., $j_x(+0)=0$) we derive condition (31) and an expansion of $\varphi(x)$ for small $x (x>0)$:

$$\varphi(x)\approx\varphi(0)\left[1+\frac{q_y\sigma_{xy}}{i\sigma_{xx}}x\right]\equiv\varphi(0)\left[1-\frac{\pi x}{lS}\right]. \tag{A12}$$

In this case the principal contribution to Q and D for $|q_y l| \ll 1$ comes from the term ρ_1 in (A10):

$$Q\equiv\int_{-\infty}^{+\infty}\rho(x)\,dx\approx\frac{\varkappa}{2}\frac{\varphi(0)}{S},\qquad D\equiv\int_{-\infty}^{+\infty}x\rho(x)\,dx\approx\frac{\varkappa}{2}\frac{l}{\pi}\varphi(0). \tag{A13}$$

If we take (A11) into account, it follows from (A13) that the first term in the expansion (A11) dominates for $x \gg |l|/\pi$ [compare with (63)]:

Let us now investigate the case of a $2D$ layer with a smooth profile in a strong magnetic field ($|l|$ is smaller than all other characteristic lengths). The principal contribution to ρ is given by the term ρ_4, which does not contain the factor l:

$$\rho(x)\approx\rho_4(x)=\frac{\varkappa}{2}\frac{\varphi(x)}{S}\frac{\partial\tilde{\theta}(x/h)}{\partial x}. \tag{A14}$$

Estimates for electrons on liquid helium ($\varphi' \lesssim \varphi/d, \tilde{\theta}' \lesssim l/h$) show that (A14) is valid for $|lS|/\pi \ll h \sim d$. Analogous estimates for heterostructures give $|lS|/\pi \ll h$.

[1]Taking into account a smooth profile for $n_s(x)$ can be important in describing EMP in real $2D$ systems at the surface of liquid helium and in MIS structures.

[2]Use of a local approximation for $\sigma_{\alpha\beta}$ limits the region of applicability of the theory developed here to the strong magnetic field side: the characteristic length over which the electric field decreases [$|lS|/\pi$ in a strong **B** field, see (47)] should exceed the cyclotron radius r_c. In the Drude model, for ω, $\tau^{-1} \ll \omega_c$ we have $r_c/l_0=\hbar\omega\varkappa/e^2(2\pi n_s)^{1/2}$. References 8, 24, and 25 used $r_c\pi/|lS| \lesssim r_c/l_0 \lesssim 0.2$.

[1]T. Ando, A. Fowler and F. Stern, *Elektronnye Svoistva Dvumernykh System* (*Electronic Properties of Two-Dimensional Systems*). Moscow: Mir, 1985 [Rev. Mod. Phys.].
[2]R. H. Ritchie, Phys. Rev. **106**, 874 (1957).
[3]F. Stern, Phys. Rev. Lett. **18**, 546 (1967).
[4]A. V. Chaplik, Zh. Eksp. Teor. Fiz. **62**, 746 (1972) [Sov. Phys. JETP **35**, 395 (1972)].
[5]T. N. Theis, Surf. Sci. **98**, 515 (1980).
[6]D. Heitman, Surf. Sci. **170**, 332 (1986).
[7]D. B. Mast, A. J. Dahm, and A. L. Fetter, Phys. Rev. Lett. **54**, 1706 (1985).
[8]S. J. Allen Jr., H. L. Störmer, and J. C. M. Hwang, Phys. Rev. **B28**, 4875 (1983).
[9]D. C. Glatti, E. Y. Andrei, G. Deville *et al.*, Phys. Rev. Lett. **54**, 1710 (1985).
[10]J.-W. Wu, P. Hawrylak, and J. J. Quinn, Phys. Rev. Lett. **55**, 879 (1985).
[11]V. A. Volkov and S. A. Mikhailov, Pis'ma Zh. Eksp. Teor. Fiz. **42**, 450 (1985) [JETP Lett. **42**, 556 (1985)].
[12]A. L. Fetter, Phys. Rev. **B32**, 7676 (1985).
[13]V. I. Tal'yanski, Pis'ma Zh. Eksp. Teor. Fiz. **43**, 96 (1986) [JETP Lett. **43**, 127 (1986)].
[14]A. L. Fetter, Phys. Rev. **B33**, 3717 (1986).
[15]A. L. Fetter, Phys. Rev. **B33**, 5221 (1986).
[16]V. A. Volkov and S. A. Mikhailov, summary of abstracts from the 4th All-Union Conference on Physical Processes in Semiconductor Heterostructures, Part 1, Minsk, 1986, p. 102.
[17]V. A. Volkov and S. A. Mikhailov, summary abstracts from the 24th All-Union Meeting on Low-Temperature Physics, Part 1, Tbilisi, 1986, p.
[18]D. C. Glatti, E. Y. Andrei, G. Deville, and F. I. B. Williams, Surf. Sci. **170**, 70 (1986).
[19]J.-W. Wu, P. Hawrylak, G. Eliasson, and J. J. Quinn, Phys. Rev. **B33**, 7091 (1986).
[20]J.-W. Wu, P. Hawrylak, G. Eliasson *et al.*, Solid State Commun. **58**, 795 (1986).
[21]J.-W. Wu, G. Eliasson, and J. J. Quinn, Solid State Commun. **58**, 799 (1986).
[22]R. P. Leavitt and J. W. Little, Phys. Rev. **B34**, 2450 (1986).
[23]S. A. Govorkov, M. I. Reznikov, A. P. Senichkov, and V. I. Tal'yanski, Pis'ma Zh. Eksp. Teor. Fiz. **44**, 380 (1986) [JETP Lett. **44**, 487 (1986)].
[24]V. A. Volkov, D. V. Galchenkov, L. A. Galchenkov *et al.*, Pis'ma Zh. Eksp. Teor. Fiz. **44**, 510 (1986) [JETP Lett. **44**, 665 (1986)].
[25]S. A. Govorkov, M. I. Reznikov, B. K. Medvedev *et al.*, Pis'ma Zh. Eksp. Teor. Fiz. **45**, 252 (1987) [JETP Lett. **45**, 316 (1987)].
[26]S. S. Nazin, N. I. Shikina, and V. B. Shikin, Zh. Eksp. Teor. Fiz. **92**, 1648 (1987) [Sov. Phys. JETP **65**, 924 (1987)].
[27]V. I. Tal'yanski, Zh. Eksp. Teor. Fiz. **92**, 1845 (1987) [Sov. Phys. JETP **65**, 1036 (1987)].
[28]E. I. Rashba and V. B. Timofeev, *Fizika i Tekhnika Poluprovodnikov* (*Semiconductor Physics and Engineering*) **20**, 977 (1986).
[29]L. A. Vainshtein, *Teoriya Difraktsiya i Metod Faktorizatsii* (*Theory of Diffraction and Factorization Methods*). Moscow: Sov. Radio, 1986, p. 12.
[30]N. March, W. Kohn, P. Vashista *et al.*, (*Theory of the Inhomogeneous Electron Gas*), S. Lundquist and N. March eds., Plenum, New York (1983), ch. 3.
[31]S. M. Apenko and Yu. E. Lozovik, Zh. Eksp. Teor. Fiz. **89**, 573 (1985) [Sov. Phys. JETP **62**, 328 (1985)].

[32]V. A. Volkov, D. V. Galchenkov, L. A. Galchenkov *et al.*, Pis'ma Zh. Eksp. Teor. Fiz. **43**, 255 (1986) [JETP Lett. **43**, 326 (1986)].
[33]F. Kuchar, R. Meisels, G. Weimann, and W. Schlapp, Phys. Rev. **B33**, 2968 (1986).
[34]D. F. Gakhov, *Kraevye Zadachi* (*Boundary-Value Problems*). Moscow: Nauka, 1977.
[35]F. D. Berkovich, Izv. Vuzov, Matematika (University Mathematics Bull.) **1**, 3 (1966).
[36]S. V. Iordansky, Solid State Commun. **43**, 1 (1982).
[37]V. T. Dolgopolov and S. I. Dorozhkin, Poverkhnost' (Surfaces) **2**, 5 (1985).
[38]R. Mehrotra, C. J. Guo, Y. Z. Ryan *et al.*, Phys. Rev. **B29**, 5239 (1984).
[39]A. P. Prudnikov, Yu. A. Brychkov, and O. I. Maruchev, *Integrals and Series*, Gordon and Breach, New York (1986).
[40]*Handbook of Special Functions*, M. Abramowitz and I. M. Stegun, U. S. Gov. Printing Office, 1964, p. 1004.

Translated by Frank J. Crowne